Università degli Studi di Padova

Dipartimento di Scienze Biomediche

SCUOLA DI DOTTORATO DI RICERCA

IN SCIENZE BIOMEDICHE

Ciclo XXXII

Impact of ER morphological alterations due to Hereditary Spastic Paraplegia mutants on Ca^{2+} homeostasis

Direttore della Scuola: Ch.mo Prof. Paolo Bernardi

Supervisore: Prof.ssa Paola Pizzo

Co-supervisore: Dr.ssa Diana Pendin

Dottorando: Nicola Vajente

Index

Summary

In eukaryotic cells, the endoplasmic reticulum (ER) extends as a network of interconnected tubules and sheet-like structures. ER tubules dynamically change their morphology and position within the cell in response to physiological stimuli and these network rearrangements depend on the microtubule (MT) cytoskeleton. Store-operated calcium entry (SOCE) relies on the repositioning of ER tubules to form specific ER-plasma membrane junctions. Indeed, the tips of polymerizing MTs are supposed to provide the anchor for ER tubules to move toward the plasma membrane. However, the precise role of ER and MT cytoskeleton during SOCE has not been conclusively clarified.

Here I exploit an *in vivo* genetic approach to alter ER morphology in the nervous system, using *Drosophila melanogaster* as a model organism. ER shape has been altered directly, by downregulating Rtnl1, the protein responsible for ER tubules formation and maintenance, or indirectly, manipulating MT dynamics, by expressing a dominant-negative variant of the MT-severing protein spastin.

I show that MT hyper-stabilization alters ER morphology, favoring an enrichment in ER sheets at the expense of tubules. Stabilizing MTs has a negative impact on the process of SOCE and results in a reduced ER calcium (Ca^{2+}) content, affecting the flight ability of the flies. Restoring proper MT organization by administering the MT-destabilizing drug vinblastine, chronically or acutely, rescues ER morphology, SOCE and flight ability.

Similarly, upon downregulation of Rtnl1, ER sheets proliferate. Moreover, SOCE is impaired and flight ability decreases. These results suggest that ER shape alteration, in particular the enrichment in cisternal components at the expenses of tubules, is the primary cause of Ca^{2+} entry reduction.

Riassunto

Il reticolo endoplasmatico (RE) si estende nelle cellule eucariotiche in una rete di cisterne e strutture tubulari. I tubuli del RE cambiano dinamicamente la loro struttura e posizione all'interno della cellula in risposta a stimoli fisiologici; questo riarrangiamento avviene grazie al citoscheletro, composto dai microtubuli (MT). Affinché l'ingresso di calcio nella cellula attivato in seguito allo svuotamento delle riserve intracellulari (SOCE) avvenga, i tubuli del RE devono essere posizionati in stretta prossimità con la membrana plasmatica (MP) per formare delle giunzioni RE-MP. Si suppone che la punta dei MT in formazione interagisca con il tubulo crescente di RE guidandolo verso la MP. Il ruolo preciso del citoscheletro durante il SOCE, tuttavia, non è ancora completamente chiarito.

In questo lavoro utilizzo *Drosophila melanogaster* come organismo modello per alterare, *in vivo*, la morfologia del RE nel sistema nervoso. La morfologia del RE viene alterata direttamente *down*-regolando la proteina Rtnl1, responsabile per la formazione ed il mantenimento dei tubuli del RE; o indirettamente, manipolando la dinamica dei MT esprimendo nei neuroni di drosofila la mutazione dominante negativa di spastina, una proteina la cui funzione è il taglio dei MT.

Nel lavoro dimostro che la iper-stabilizzazione dei MT altera la morfologia del RE favorendo la componente composta da cisterne alle spese della componente tubulare. Questa stabilizzazione dei MT ha un impatto negativo nel processo del SOCE, causando una riduzione della quantità di calcio intracellulare, che va a diminuire la capacità di volare delle drosofile. Il ripristino dell'organizzazione ottimale dei MT, tramite somministrazione cronica o acuta di vinblastina, un farmaco che destabilizza i MT, recupera la morfologia del RE, il SOCE e la capacità di volare. Similarmente, *down*-regolando Rtnl1 la componente di cisterne del RE prolifera, il SOCE è alterato e la capacità nel volo diminuisce. Questi risultati suggeriscono che l'alterazione nella morfologia del RE, in particolare l'arricchimento della componente di cisterne alle spese della componente tubulare, è la causa primaria della riduzione del SOCE.

Introduction

Endoplasmic reticulum (ER)

ER structure and organization

ER is a multifunctional organelle that coordinates a variety of cellular processes fundamental for cell life. These include translocation of secretory proteins, integration of proteins into the membrane, protein folding and modification, synthesis of phospholipids and steroids, storage of Ca^{2+} ions and their regulated release into the cytosol (Figure 1A).

The interphase ER can be divided into nuclear and peripheral ER. The nuclear ER, or nuclear envelope (NE), consists of two sheets of membranes with a lumen. The NE surrounds the nucleus, with the inner and outer membranes connecting only at the nuclear pores and is underlaid by a network of lamins. The peripheral ER is a network of tubules and sheet-like structures that extend throughout the cell cytoplasm. The luminal space of the peripheral ER is continuous with that of the nuclear envelope and together they comprise >10% of the total cell volume (Terasaki and Jaffe, 1991). Several works have proven the continuity of the ER network. As an example, experiments of Fluorescence Loss In Photobleaching (FLIP) using GFP-tagged proteins targeted either to the ER lumen or membrane demonstrated that upon continuous photo-bleaching of a selected region, the fluorescence of the entire membrane network is depleted (Dayel et al., 1999) (Figure 1B).

The ultrastructure of the ER has been visualized by electron microscopy (EM) in several cell types. Within the peripheral ER, the most obvious difference observed is between rough, i.e. ribosome-studded, and smooth regions (RER and SER, respectively). Historically, ER cisternae have been classified as ribosome bound, “rough” ER, while ER tubules are considered ribosome-free,

“smooth” ER. The purpose of differently shaped ER domains remains a subject of debate. Cisternae have a larger luminal volume and surface area than tubules, suggesting that they would be the preferred site for luminal processes like protein folding (Puhka et al., 2012; Shibata et al., 2010; West et al., 2011). Consistent with this idea, during the ER stress response yeast peripheral ER shows increased cisternae to accommodate an increase in protein folding (Schuck et al., 2009). ER tubules have lower luminal volume to surface area than cisternae, suggesting that ER tubules could be the preferred site for the accumulation of integral membrane proteins and for processes connected to lipid synthesis (West et al., 2011). Also, the relative abundance of RER and SER found among different cell types correlates with their functions. For example, cells that secrete a large percentage of their synthesized proteins contain mostly RER. Nevertheless, there are many examples of ER tubules that do have bound ribosomes, just at a lower density than cisternae, indicating that they are not always ribosome excluded (Puhka et al., 2012; West et al., 2011). Accordingly, recent evidence suggests that the separation between tubules and cisternae is not clear-cut. Structural analysis performed on EM sections of HeLa cells shows the transformation of long cisternae into tubules during mitosis occurs via a progressive formation and expansion of fenestration (Puhka et al., 2012). 3D tomograms obtained from TEM thin-sections of Vero and HeLa cells showed that these fenestrated sheets are visible in 2D sections in the shape of long ER profiles separated by small gaps (Lu et al., 2009). Moreover, recent findings indicate that peripheral cisternae are in part composed of clusters of highly dense peripheral tubules. These structures, traditionally seen as cisternae due to limited spatiotemporal resolution, are proposed to be in part responsible for promoting the high dynamicity of the peripheral ER. Indeed, the fast rearrangement of the peripheral ER is due to the rapid interconversion between loose and tight polygonal arrays of tubules, enabling the ER to rapidly reconfigure its spatial footprint in response to intracellular stimuli (Nixon-Abell et al., 2016).

Recent observations using STimulated Emission Depletion (STED) super-resolution microscopy confirmed that in living cells ER is not limited to uniform sheets and tubules but instead contains a continuum of membrane structures that

includes highly dynamic “nanoholes” within sheets and clustered tubules. Dynamic nanoscale morphology of the ER surveyed by STED microscopy (Schroeder et al., 2019).

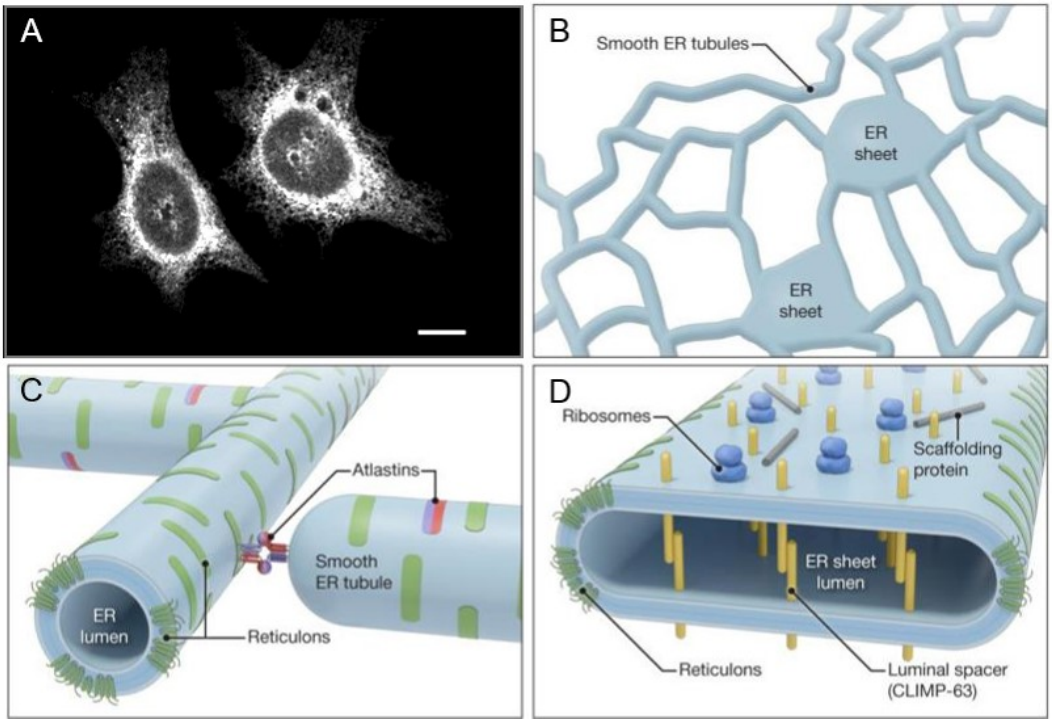

Figure 1. Mechanisms involved in ER network shaping. **(A)** ER network of HeLa cells visualized with the luminal marker sfGFP-KDEL. Scale bar: 10 µm. **(B)** Diagram showing interconnection between smooth ER tubules and sheets. **(C)** ER shaping proteins: reticulons and atlastins on ER tubules. **(D)** ER proteins involved in formation and stabilization of ER sheets. Scaffolding proteins include p180 and kinectin. Adapted and modified from (Goyal and Blackstone, 2013).

Formation and maintenance of the network: ER dynamics

In recent years, many advances have been made in understanding how the architecture of the ER is formed and maintained. ER network is very dynamic: it is continuously remodeled, while maintaining its characteristic structure. ER tubules continuously form, retract and slide along microtubules (MTs), a process facilitated by associated molecular motors and dynamic changes of the cytoskeleton. The purpose of the constant reorganization of the tubular ER network is not completely understood; however, it is reasonable to think that ER

dynamics are instrumental for specific ER function, *i.e.* facilitating organelle contact for exchange of proteins, lipids, and Ca^{2+} (Baumann and Walz, 2001; English et al., 2009). A few basic processes contribute to ER dynamics, including fusion, fission, elongation, retraction and branching of tubules, ER-phagy.

Membrane tubules are important structural elements of the ER (Dreier and Rapoport, 2000; Lee et al., 1989); their diameter varies between 50–100 nm, whether formed *in vitro* or *in vivo*, and it is conserved from yeast to mammalian cells, indicating that their formation is a regulated and fundamental process.

Two evolutionarily conserved protein families, the reticulons (Rtns) and REEPs (Voeltz et al., 2006), are responsible for shaping ER tubules. They are ubiquitous membrane proteins that are both necessary and sufficient to generate tubules (Hu et al., 2008). How these proteins generate and stabilize membrane curvature is still unclear (see below). One of Rtns (Rtn-3) has also been implied in ER-phagy, a remodelling process in which discrete fragments of the ER are enwrapped inside the autophagosomes and degraded via the lysosomal machinery (Grumati et al., 2017).

Connecting tubules into a network requires homotypic membrane fusion of ER tubules. This process is essential for preserving the typical structure of the ER (Vedrenne and Hauri, 2006), and its failure prevents the formation of an intact ER network (Dreier and Rapoport, 2000). ER membrane fusion is carried out by the Atlastin (Atl) family of dynamin-like GTPases (Anwar et al., 2012; Hu et al., 2009; Orso et al., 2009; Rismanchi et al., 2008). Mammals have three closely related Atls. These proteins contain a cytoplasmic GTPase domain, followed by a three-helix bundle, a membrane-bound hairpin region and an amphipathic C-terminal tail (Betancourt-Solis et al., 2018). Depletion of endogenous single fly hortologue of Atls causes the fragmentation of ER tubules, as a result of the absence of membrane fusion (Hu et al., 2009; Orso et al., 2009) (Figure 1C).

The fusion of ER tubules generates three-way junctions, which are small, triangular sheets with negatively curved edge lines (Shemesh et al., 2014). It has been suggested that these junctions are stabilized by the lunapark protein (Chen

et al., 2012, 2015; Shemesh et al., 2014), a conserved membrane protein containing two closely spaced TM segments.

Less is known regarding how peripheral ER cisternae are shaped. Although it is clear that ER cisternae can be propagated by the depletion of Rtns (Anderson and Hetzer, 2008; De Craene et al., 2006; Shibata et al., 2010; Voeltz et al., 2006; West et al., 2011), other factors are involved in cisternae generation. One idea is the involvement of polyribosomes associated with translocation complexes, a structure thought to help stabilize the flat membrane regions of the cisternae (Puhka et al., 2007; Shibata et al., 2006). In support of this theory, addition of drugs that dislocate polyribosomes from ER membranes causes a reduction in the amount of cisternal peripheral ER (Puhka et al., 2007). Conversely, the amount of cisternal peripheral ER increases when an integral ER membrane protein that binds ribosomes, p180, is overexpressed (Benyamini et al., 2009; Shibata et al., 2010). In general, sheets formation is stimulated by coiled-coil containing membrane proteins such as p180, kinectin and CLIMP-63, with the latter forming luminal bridges between the juxtaposed membranes (Shibata et al., 2010) (Figure 1D).

ER in neurons

ER network spawn across the entire cell body, reaching almost every part of it. Some cell types, *e.g.* neurons, need tweaks and adjustments of ER structure due to their specialized shape or function. Neurons are characterized by the compartmentalization into functional modules, *i.e.* cell bodies, dendrites and axons. The morphology of ER in these compartments is a consequence of their form and function. Indeed, neuronal cell bodies contain both SER and RER, which exhibit dynamic transition between each other (Hanus and Ehlers, 2016). Stacked sheets are connected by helicoidal structures, providing an extended surface for ribosomes (Terasaki et al., 2013), necessary for protein translation.

Dendrites and axons are responsible for the transmission of signals across the network. In contrast to the sheet-like structures in cell bodies and dendrites,

axonal ER is primarily tubular, with an enrichment in a population of very narrow tubules (~20-30 nm in diameter) (Terasaki, 2018). RER constitutes a very small fraction of axonal ER (O'Sullivan et al., 2012), suggesting a limited contribution of ER-associated ribosomes in axonal protein translation. The axonal subpopulation of narrow tubules do not connect together in three-way junctions as in cell bodies, probably because of curvature constraints given by the small diameter. Instead, they connect at the edges of sheets with high curvature (Terasaki, 2018).

Microtubules (MTs)

MTs are dynamic polarized cytoskeletal components implicated in a wide range of cellular processes: intracellular transport, organelle positioning, chromosome separation during cell division, regulation of cell polarity and morphogenesis and formation of cilia and flagella basis. In most cells, MTs nucleate from the MT-organising centre (MTOC) and expands through the cytoplasm.

MTs formation

MTs form through the dynamic polymerization in proto-filaments of αβ-tubulin heterodimers. The polymerization occurs in a head to tail fashion to form a highly polarized structure with a plus end exposing α-tubulin and a minus end exposing β-tubulin (Kapitein and Hoogenraad, 2015). Assembly requires β-tubulin to be in its guanosine triphosphate (GTP)-bound form; the rapid hydrolysis into guanosine diphosphate (GDP) upon incorporation into the MT lattice generates a GTP-cap at the plus-end, favoring further polymerization. It is widely accepted that the growing MT tip contains the GTP-cap, which has stabilizing properties, whereas the MT shaft is composed of GDP-bound tubulin and is intrinsically unstable. The GTP-cap model explains the dynamic nature of MTs: in the presence of the cap, a MT continues growing, exploring and probing the intracellular space; loss of the cap, instead, leads to rapid MT shrinkage (Desai and Mitchison, 1997).

At the structural level, GTP hydrolysis: i) triggers conformational changes in α-tubulin, leading to global lattice rearrangements and generation of lattice strain (Alushin et al., 2014; Hyman et al., 1995; Zhang et al., 2015); ii) allosterically affects lateral contacts between protofilaments (Yajima et al., 2012).

Both the MT plus end (at which β-tubulin is exposed) and the MT minus end (at which α-tubulin is exposed) can grow in solutions of purified tubulin and thus can bear a GTP cap. However, the dynamic properties of the two ends are markedly different: the minus end grows more slowly and undergoes catastrophe less frequently than does the plus end. The two MT ends also behave differently when the stabilizing cap is severed in vitro: the plus end depolymerizes, whereas the minus end remains relatively stable and can resume growth (Mandelkow et al., 1991; Tran et al., 1997).

MTs dynamics

Thanks to their highly dynamic structure, MTs undergo cycles of rapid growth and disassembly in a process defined as dynamic instability (Kapitein and Hoogenraad, 2015). This dynamic instability, which occurs mainly at the MT plus-ends, provides a rapid reorganization of the cytoskeleton that is necessary for many cellular functions, such as cell division and migration and formation of cell polarity.

The switch from growth to disassembly (or shrinkage) is called “catastrophe”, while the reverse is termed “rescue”; both these dynamic mechanisms are complex and poorly understood. *In vitro* works show that MTs that have been growing for a longer time (‘older’ MTs) have a higher chance of undergoing a catastrophe. This ‘ageing’ behaviour suggests that the induction of catastrophe requires several molecular events to occur before a MT switch to depolymerization (Gardner et al., 2011; Odde et al., 1995). The nature of these catastrophe-promoting events is unknown, but they might involve the accumulation of MT-lattice defects or an increased tapering of the growing MT end (Coombes et al., 2013; Gardner et al., 2011). In cells, catastrophes can be

triggered by the exertion of different obstacles, such as the cell cortex, which slow down MT growth and lead to the loss of the GTP cap and an eventual catastrophe (Janson et al., 2003).

MT rescues are understood even less well than catastrophes. Their occurrence *in vitro* is not sensitive to tubulin concentration (Walker et al., 1988) and thus might not depend on the stochastic addition of GTP-tubulin dimers to the shrinking MT plus end. Instead, rescues might be induced by local lattice features that can halt MT disassembly, such as 'GTP islands' of GTP-tubulin that mimic the stabilizing GTP cap (Dimitrov et al., 2008) (Figure 2A).

The MT dynamicity is affected also by post-translational modification (PTM). PTM occurs preferentially on the αβ-tubulin heterodimers of stable MTs changing their properties and functions (Hammond et al., 2008; Janke and Kneussel, 2010; Wloga and Gaertig, 2010). These PTM are able to alter the MT dynamics by increasing or decreasing their stability, ability to polymerize and functionality. Modifications that are associated with increased stability are detyrosination and acetylation. Tubulin phosphorylation is involved in a still unclear way to MTs assembly and disassembly (Wandosell et al., 1987). Ubiquitination of tubulin inhibits MT formation and polymerization (Schaefer et al., 2012) while tubulin polyglutamylation can modulate the functional specificity of MT subpopulations (Boucher et al., 1994; Ikegami et al., 2007).

Neuronal axons are prime examples of a mixed population of MTs due to PTMs. In fact, the outgrowing neuronal axon is composed of a labile and dynamic domain at the distal end, enriched in tyrosinated MTs. Conversely, at the proximal end of the axon, there is a stable domain enriched in detyrosinated and acetylated tubulin (Fukushima et al., 2009; Perdiz et al., 2011; Witte et al., 2008). These observations led to the hypothesis that MT dynamics differ throughout the axon and growth cone of neurons (Fukushima et al., 2009; Hammond et al., 2008; Janke and Kneussel, 2010; Wloga and Gaertig, 2010).

In mature neurons, acetylated MTs are non-uniformly distributed with enrichment in the proximal region of axons and present at decreased levels in the cell body,

dendrite, and growth cone. Conversely, in young neurons, acetylated MTs are in the proximal regions of the neurites and cell body undergoing neurite outgrowth.

Although the causal link between tubulin PTMs and MT stability remains largely enigmatic, PTMs need to be accurately regulated since the consequences of their dysregulation are detrimental for neuronal health (Erck et al., 2005).

MT dynamics not only derives from spontaneous polymerization/collapse and PTMs, but is also actively controlled through the activity of specific proteins (see below).

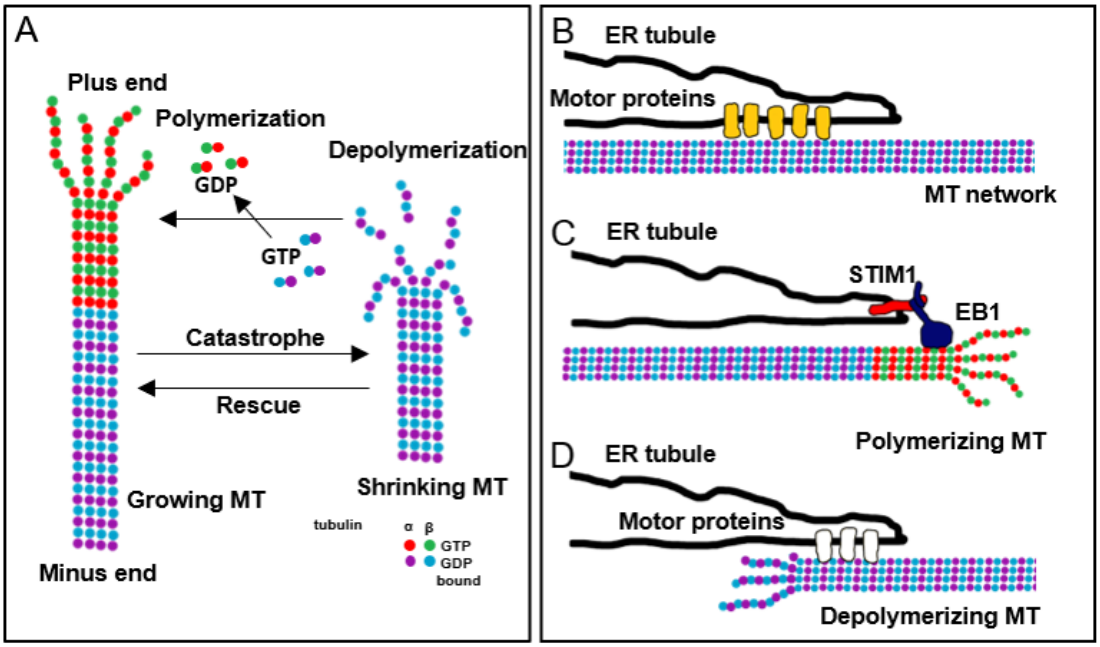

Figure 2. (A) The cycle of tubulin assembly (polymerization) and disassembly (depolymerization) is powered by hydrolysis of the GTP bound to β-tubulin, which enables MTs to switch between catastrophes and rescues. GTP-bound tubulin dimers are incorporated into polymerizing MTs. GTP hydrolysis occurs after a GTP-tubulin dimer incorporates into the structure of growing MT tips. The loss of the stabilizing GTP cap leads to a catastrophe and rapid depolymerization. **(B, C, D)** Scheme of the processes implicated in the extension and positioning of ER tubules. **(B)** ER tubules can extend along pre-existing MTs in a process termed sliding, which can be driven by MT-based molecular motors. **(C)** An ER tubule can be formed when a membrane attaches to the plus end of a growing MT via a membrane-MT tip attachment complex (TAC). **(D)** ER tubules can be pulled by depolymerizing MT ends (dTAC).

MT-related ER dynamics

Experiments in *Xenopus* egg extracts or proteoliposomes have shown that the cytoskeleton is not necessary for the formation of ER tubular network *in vitro*. The process of ER network formation is not affected by the addition of inhibitors of MT polymerization, by the depletion of tubulin from the extract or by inhibitors of actin polymerization (Dreier and Rapoport, 2000). Indeed, rececent evidence showed that a small set of membrane proteins (Sey1p/Atl, Yop1p/Rtnl1) inserted in proteoliposomes are sufficient to form an ER network *de novo* (Powers et al., 2017). Nevertheless, several studies report a role of the cytoskeleton in the maintenance of ER dynamics.

In different cell types, ER tubules have been demonstrated to co-align with MTs (Guo et al., 2018). A role for MTs has been confirmed in ER tubules movement. MT-based ER tubules dynamics have been studied with time-lapse microscopy and three distinct mechanisms have been identified: i) tip attachment complex (TAC); ii) ER sliding (Lee and Chen, 1988; Waterman-Storer and Salmon, 1998) and iii) depolymerization of MT ends (dTAC) (Guo et al., 2018)

(i) TAC dynamics occur when a membrane attaches to the plus end of a growing MT via a membrane-MT tip attachment complex (Grigoriev et al., 2008; Guo et al., 2018; Waterman-Storer et al., 1995; Waterman-Storer and Salmon, 1998). The minimal requirements for TAC are: End Binding (EB) proteins, which recognize the stabilizing cap at growing MT ends (Maurer et al., 2012), and the ER-resident transmembrane protein STromal Interaction Molecule (STIM1) (Grigoriev et al., 2008). TAC movements depend on the tethering between EB1 and STIM1 due to its EB-binding MT Tip Localization Sequence (MTLS). STIM1 and other proteins containing an MTLS can interact with MTs not only though EBs, but also directly, by binding to the negatively charged MT surface (Honnappa et al., 2009) (Figure 2B).

(ii) ER tubules can also extend along pre-existing MTs in the process called sliding. It is a process driven by MT-based molecular motors that involves kinesin and dynein (Friedman et al., 2010; Grigoriev et al., 2008; Waterman-Storer and Salmon, 1998; Woźniak et al., 2009). The extraction of membrane tubes moving

on stabilized MTs has been extensively studied by *in vitro* reconstitution experiments (Campàs et al., 2008; Koster et al., 2003; Leduc et al., 2004; Roux et al., 2002; Shaklee et al., 2008). However, it is still not clear how MT-based motors attach to the ER and the extension of its contribution on ER tubulation in cells (Figure 2C).

(iii) The molecular mechanisms underlying dTAC, a recent discovery in membrane-MT tubulation dynamics, are currently unknown and it is unclear whether dTACs can be driven by the same molecules that are responsible for TAC (Guo et al., 2018) (Figure 2D).

Each of these mechanisms can lead to tubule extension and, when tubules intersect, they fuse and create three-way junctions (Allan and Vale, 1991; Waterman-Storer and Salmon, 1998). Recent experiment suggests that this continuous rearrangement of ER network and the dynamics of the three-way junctions (Powers et al., 2017) may promote the rapid adaptation of ER shape to different conditions.

Despite the cytoskeleton contributes to ER dynamics, it is not clear whether it is necessary for the maintenance of a pre-existing ER network. Several observations suggest that in mammalian cells MT cytoskeleton dynamics influence ER tubules distribution and sheet/tubule balance (Dabora and Sheetz, 1988; Lee and Chen, 1988; Lu et al., 2009; Terasaki et al., 1986; Waterman-Storer and Salmon, 1998. Depolymerization of MTs by nocodazole in mammalian tissue culture cells inhibits new tubule growth and causes retraction of ER tubules from the cell periphery (Guo et al., 2018; Terasaki et al., 1986). Moreover, it is known that ER growth along MTs allows the organelle to populate the entire surface of cells as well as the length of axons (Farías et al., 2019).

Store-operated Ca^{2+} entry (SOCE)

The main source of Ca^{2+} for ER refilling is the extracellular milieu, and ER tubules contact the plasma membrane (PM) in a process called SOCE, which serves to

generate a sustained cytosolic Ca^{2+} elevation and refill the depleted ER Ca^{2+} stores (Terasaki et al., 2001; Wu et al., 2006).

The molecular players involved in SOCE include the pore-forming subunit of the Ca^{2+}-release activated Ca^{2+} channel encoded by the Orai gene (Feske et al., 2006; Prakriya et al., 2006; Vig et al., 2006a, 2006b; Yeromin et al., 2006; Zhang et al., 2006a) and the ER-resident protein STIM (Liou et al., 2005; Zhang et al., 2005), that serves as a lumenal Ca^{2+} sensor (Friedman et al., 2010; Grigoriev et al., 2008; Soboloff et al., 2012). It has been demonstrated that after Ca^{2+} store depletion, STIM oligomerizes and redistributes to predetermined foci in the peripheral ER (Luik et al., 2008). STIM binds the MT plus-end binding protein EB1, which facilitates TAC-dependent STIM translocation towards the PM (Chen et al., 2013; Honnappa et al., 2009; Liou et al., 2007; Tsai et al., 2014). At the ER–PM junctions, STIM interacts with Orai channels to promote influx of extracellular Ca^{2+} into the ER (Galán et al., 2011; Grigoriev et al., 2008; Liou et al., 2007).

An intact, functional and mobile ER is required for STIM to reach out to the PM and form new ER-PM junctions (Carrasco and Meyer, 2011; Wu et al., 2006). This indicates that two main players are necessary: ER tubules and MT cytoskeleton. The role of cytoskeleton on SOCE is indirect, indeed it provides to the ER the support for its movement. The precise role of TAC-based ER motility in this reorganization, however, is still controversial and appears to vary among cell types (Galán et al., 2011; Grigoriev et al., 2008; Redondo et al., 2006; Smyth et al., 2007). A current model suggests that TAC-mediated ER movement is required prior to SOCE activation to appropriately position STIM throughout the ER, with ER Ca^{2+} depletion causing MT-independent STIM translocation to the PM. Although the molecular details of this process are unclear, local cytoskeleton reorganization likely plays a role (Smyth et al., 2007) (Figure 3).

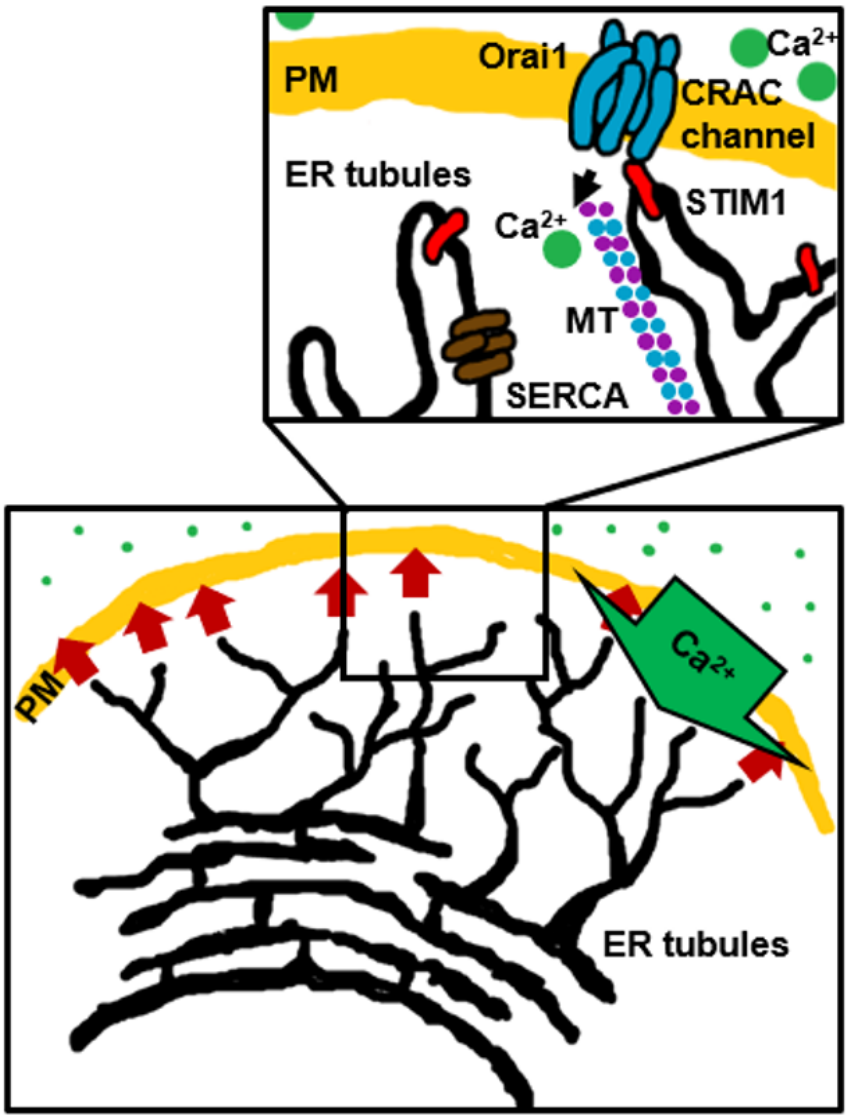

Figure 3. Graphic representation of SOCE mechanism. STIM1 protein senses the decreased ER calcium concentration ($[Ca^{2+}]_{ER}$), promoting the movement of the ER tubules towards the PM along MTs. STIM1 interacts with Orai1 promoting its oligomerization to form the CRAC channel. Ca^{2+} enters through the CRAC channel, transiently increasing the cytosolic calcium concentration ($[Ca^{2+}]_c$) and replenishes ER through SERCA pump.

Hereditary spastic paraplegia

Hereditary spastic paraplegia (HSPs) are inherited disorders with an incidence of 1.8/100000 (Ruano et al., 2014). The major clinical signs of the disease are progressive lower limb spasticity and weakness. Post-mortem studies on HSP patients revealed distal-end degeneration of ascending sensory fibres and

corticospinal tract axons. The genetic of HSP comprises a variety of mutations in more than 70 distinct loci with more than 60 gene products mutated (Lo Giudice et al., 2014; Novarino et al., 2014). While with diverse functions, proteins encoded by HSP genes cluster within a small number of predicted cellular activities, such as: membrane traffic and organelle shaping, mitochondria regulation, myelination and lipid/sterol modification, axonal path-finding and axonal transport. Whether or not mutations in HSP genes produce the pathology by a common mechanism remains unknown. Interestingly, despite the genetic heterogeneity of HSPs, alterations in morphology and/or distribution of the ER appear to be a critical causative factor, as over 60% of HSP patients carries mutations in genes encoding proteins that act on ER morphology, either directly or affecting its cellular distribution (Fink, 2013; Lo Giudice et al., 2014).

SPG4/Spastin

About 40% of autosomic dominant HSP and about 20% of sporadic HSP are caused by mutations in *SPG4/SPAST* gene, encoding spastin (Hazan et al., 1999). The *SPAST* gene spans a region of 90 kb in genomic DNA and comprises 17 exons. Most SPG4 patients show a pure phenotype, which is characterized by muscle weakness and bladder dysfunction, with average onset in the fourth decade of life, variably accompanied by column sensory deficits and different phenotypic variation (McDermott et al., 2006; Orlacchio et al., 2008; Schulte et al., 2003).

Over 300 mutations, including partial deletions, have been described; all pathogenic gene variants affect the AAA domain. Loss-of-function mechanisms (haploinsufficiency or dominant-negative) have been proposed for the disease (Beetz et al., 2006). Haploinsufficiency and dominant-negative are two different mechanisms characterized by insufficient functional proteins. In case of haploinsufficiency insufficient levels of functional protein are present (because the mutated protein is present but not functional or because the mRNA or protein is unstable). In case of the dominant-negative mechanism, the dysfunctional mutant protein interacts with the wild-type (WT) protein impairing its function.

Spastin protein is a major player in MTs regulation. Spastin is a MT-severing protein, member of the AAA (ATPase associated with various cellular activities) protein family. The spastin AAA cassette contains three conserved ATPase domains, including: Walker motif A, corresponding to the ATP-binding domain; Walker motif B and the AAA minimal consensus sequence (Hazan et al., 1999).

Spastin breaks long MTs into shorter ones, thereby regulating the number and mobility of MTs and the distribution of their dynamic plus-ends (Baas et al., 2006; Errico et al., 2002; Evans et al., 2005; Roll-Mecak and Vale, 2005). To sever MTs, spastin needs to assemble into hexamers, dock on MTs and break them by pulling the negatively charged C-terminal of tubulin through the central pore of the hexamer (Roll-Mecak and Vale, 2008; White et al., 2007). Spastin hexamers sever preferentially the stable region of axonal MTs by targeting PTM (Lacroix et al., 2010; Valenstein and Roll-Mecak, 2016). Consistent with this, knockdown of spastin tends to shift the MT mass of the axon toward a higher proportion of the more stable regions (Riano et al., 2009) (Figure 4A).

SPAST open reading frame has two initiation codons (Claudiani et al., 2005) preceded by two Kozak sequences: a weak one surrounding the M1 initiation and a stronger one before the M87 initiation codon (Claudiani et al., 2005; Kozak, 2002). As a result, a 616 amino acid (68 kDa) isoform called M1 and a 530 amino acid (60 kDa) isoform called M87 are synthesized simultaneously but at different levels. The MIT, MTBD and AAA domains are present in both M1 and M87 spastin isoforms, whereas the 86-amino acid N-terminal domain is present only in M1 spastin. Analysis of spastin expression in adult human CNS has revealed the presence of M87 both in spinal cord and cerebral cortex, whereas significant levels of M1 were detected only in spinal cord and not in brain (Solowska et al., 2010). The M1 hydrophobic region has been suggested to form a hairpin that can partially insert into ER membrane. It is however unclear whether M1 spastin inserted into ER membrane would participate with the cytosolic one to exert its ATPase activity.

Spastin hydrophobic hairpins have been reported to interact with ER resident proteins Atl-1, Rtn-1 and REEP1 (Blackstone et al., 2011; Evans et al., 2006;

Mannan et al., 2006; Park et al., 2010; Sanderson et al., 2006). The three proteins have been involved in the morphogenesis of ER, suggesting that their coordinated interaction could be important for ER–MT interactions that build the tubular ER network (Blackstone, 2012; Blackstone et al., 2011; Lumb et al., 2012; Park et al., 2010).

One example of mutation in spastin protein causing a dominant-negative effect is the substitution K388R. A Drosophila model expressing spastin carrying K467R mutation has been previously generated and characterized (Orso et al., 2005). In order to exert MT-severing activity, spastin form hexamers (Eckert et al., 2012; Pantakani et al., 2008). When mutated, the protein could co-hexamerize with the WT one, thus forming a dysfunctional hexamer while subtracting part of the functional WT spastin. Accordingly, when spastin^{K467R} is expressed in flies nervous system, neuronal MTs are hyper-stabilized, a phenotype reminiscent of that observed upon spastin downregulation (Orso et al., 2005).

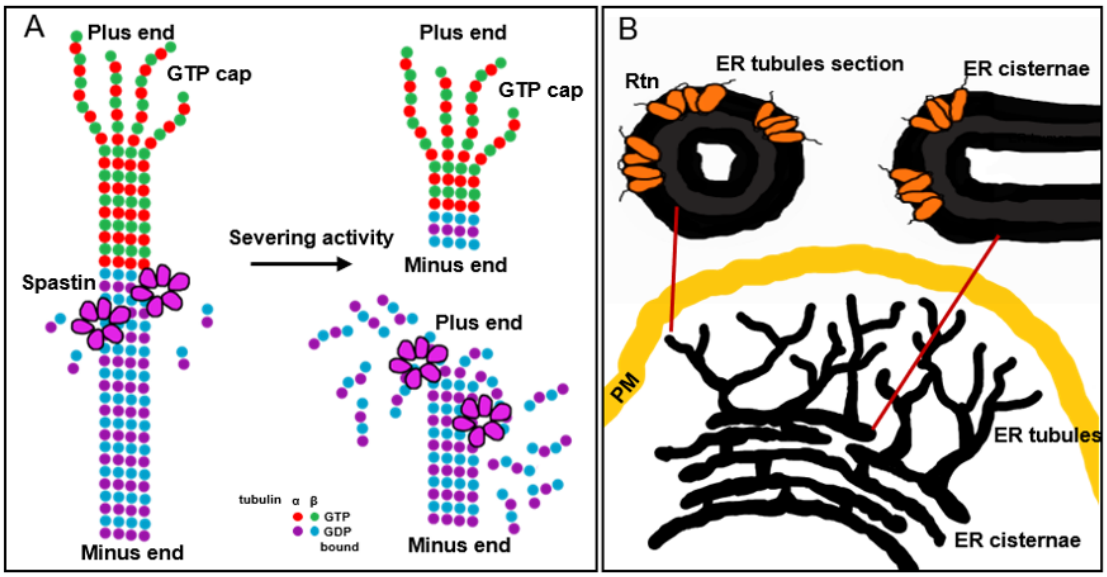

Figure 4. (A) Graphic representation of spastin severing activity, spastin assemble into hexamers, dock on the stable region of MTs and break them by pulling the negatively charged C-terminal of tubulin through the central pore of the MT. Spastin activity induces MT catastrophe and depolymerization. **(B)** graphic representation of Rtn function. Rtns are enriched and oligomerize into ER tubules and the edges of cisternae thus promoting stabilization of high curvature membrane by formation of its typical wedge conformation.

SPG12/Reticulon

SPG12 encodes Reticulon-2 (Rtn2), one of the four mammalian paralogues of the Rtns (Montenegro et al., 2012). Mutations found in SPG12 HSP patients are frameshift, missense, and whole gene deletions, presumably leading to haploinsufficiency. The HSP form induced by SPG12 mutations is pure and with rapid progression (Orlacchio et al., 2002).

Rtns are involved in the shaping of the tubular ER (see above). All the members of Rtn family contain a uniquely conserved C-terminal domain, called Reticulon Homology Domain (RHD). The RHD is composed by two hydrophobic domains, a loop region and a short N-terminus (Chiurchiù et al., 2014). The two hydrophobic regions are too long to span the membrane once and too short to make a double pass hairpin. It has been proposed that TMDs form a particular wedge-like structure that inserts only into the ER membrane occupying only the external leaflet, causing the increase of its surface compared with the opposing leaflet (Anderson and Hetzer, 2008; Audhya et al., 2007; De Craene et al., 2006; Tolley et al., 2008; Voeltz et al., 2006).

Rtns are enriched in high-curvature ER subdomains, *i.e.* tubules, edges of cisternae and edges of fenestrations (Kiseleva et al., 2007; Schuck et al., 2009; Shibata et al., 2010). This specific localization is promoted by the RHD and is consistent with Rtns role in stabilizing high curvature ER domains (Voeltz et al., 2006)(Hu et al., 2008) necessary to form and maintain the tubular ER (Figure 4B). The role of Rtns in shaping tubular ER has been proven in different experimental systems, where overexpression of Rtn abolishes peripheral ER sheets leading to formation of long tubular ER while loss of the protein causes an expansion of cisternae (Sparkes et al., 2010; Voeltz et al., 2006; West et al., 2011) .

Drosophila models for loss of Rtn have been created by downregulating fly homologue Reticulon-like protein 1 (Rtnl1) or by disrupting endogenous Rtnl1 gene. ER sheet expansion has been observed also in these models, together

with partial loss of ER from distal motor axons, and occasional discontinuities in axonal ER (O'Sullivan et al., 2012; Yalçın et al., 2017).

Drosophila as a Research Animal Model

The path of Drosophila as a research model is a history of groundbreaking achievements, underpinned by 6 Nobel Prizes since 1933. The first went to Thomas Hunt Morgan, who delineated the theory of inheritance by using Drosophila to define genes location on chromosomes (Bridges and Morgan, 2012). Some years later, Hermann Muller defined the effects of X-rays on mutation rate in fruit flies (Muller, 1928) opening the field to modern genetics. These seminal discoveries allowed the generation of genetic tools that still prosper, e.g., balancer chromosomes, special chromosomes that, preventing meiotic crossing-over, are used to maintain complex stocks with multiple mutations on single chromosomes over generations (Zimm, 1992). New genetic tools developed over the years allowed the fruit fly to move with times. As a significant example, CRISPR/Cas9 genome editing strategies allow simple and rapid engineering of the fly genome (Ewen-Campen et al., 2017). What makes Drosophila the model organism of choice of many researchers is the observation that relevant genes, cellular processes and basic building blocks in cellular and animal biology are conserved between flies and mammals (Yoshihara et al., 2001). Moreover, compared to vertebrate models, Drosophila has considerably less genetic redundancy, making the characterization of protein function less complicated. The function of a gene product can be inferred by generating fly lines for its up- or down-regulation and then analyzing the resulting phenotypes. The fruit fly represents also an ideal model organism to study human diseases. Remarkably, over 60% of known human disease-causing genes have a fly orthologue (Wangler et al., 2015). Most of the cellular processes known to be involved in human disorders pathogenesis, including apoptosis signaling cascades, intracellular Ca^{2+} homeostasis, as well as oxidative stress, are conserved in flies. Of note, the high accessibility of the nervous system at different developmental stages, makes also neuroscience experiments feasible

in the fly model. Moreover, flies exhibit complex behaviors and, like in humans, many of these behaviors, including learning, memory and motor ability, deteriorate with age (Mockett et al., 2003; Simon et al., 2006).

Drosophila: Advantages

Beside genetics, the strongest selling point of using Drosophila as an animal model are: (i) Drosophila are relatively inexpensive and easy to keep, as they are raised in bottles or vials containing cheap jelly-like food. (ii) Generally, there are very few restrictions, minimal ethical and safety issues on their laboratory use. (iii) Flies life cycle is very fast, lasting about 10–12 days at 25 ◦C. Newly laid eggs take 24 h to undergo embryogenesis before hatching into first instar larvae, which develop into second, and then third instar larvae. The duration of these stages varies with the temperature: at 20 ◦C, the average length of the egg-larval period is 8 days; at 25 ◦C it is reduced to 5 days. Larvae transform into immobile pupa, undergo metamorphosis and eclose in the adult form 5–7 days later. (iv) A single fly can produce hundreds of offspring within days, thus it is relatively easy to quickly generate large numbers of embryos, larvae or flies of a given genotype. Individual flies are easily manipulated when anaesthetized with carbon dioxide, allowing identification of selectable phenotypic features under a stereomicroscope (Stocker and Gallant, 2008).

Drosophila: Ca^{2+} Toolkit

Ca^{2+} is the major intracellular messenger, mediating a variety of physiological responses to chemical and electrical stimulations. Therefore, cell Ca^{2+} concentration [Ca^{2+}] must be tightly controlled in terms of both space and time, a task that is accomplished by several Ca^{2+} transporting and buffering systems. Easily accessible knock-down and knock-out strategies, applicable to cell lines, as well as to living animals, have helped discovering in flies a number of molecules involved in Ca^{2+} signaling. As in mammals, basal cytosolic Ca^{2+} levels are controlled in flies by the interplay of Ca^{2+} transport systems, localized in the

plasma membrane (PM) and the membranes of intracellular organelles that function as internal Ca^{2+} stores (Figure 5). This toolkit, together with a number of Ca^{2+}-binding proteins, concurs in creating and regulating the dynamics and spatial localization of Ca^{2+} signals. The major players in Ca^{2+} signaling in Drosophila are briefly described below; the interested reader is referred to a more extensive review on the topic (Chorna and Hasan, 2012). Ca^{2+} enters the PM through Ca^{2+} channels, e.g., voltage- and ligand- gated. As for voltage-gated Ca^{2+} channels, the fly genome encodes three α1 subunits (Ca-α1D, cacophony, Ca-α1T) forming Cav1, Cav2, and Cav3 type channels, respectively, mainly expressed in the nervous system and muscles (Chorna and Hasan, 2012). Among ligand-gated channels, glutamate-gated ionotropic receptors (iGluRs) are represented in Drosophila by 15 genes encoding different subunits. As in other animal species, Drosophila uses glutamate as a fast neurotransmitter in neuromuscular junctions (NMJs), and highly Ca^{2+} permeable iGluRs are clustered in active zones in postsynaptic motor neuron terminals (DiAntonio, 2006). Cations enter sensory neurons through Transient Receptor Potential (TRP) channels. The gene encoding the first member of the trp superfamily was identified in Drosophila photoreceptors as a PM Ca^{2+} permeable channel, required for mediating the light response (Hardie and Minke, 1992). A vast number of trp homologs were found in vertebrates that have been classified in seven major subfamilies in metazoans. Cytosolic Ca^{2+} increase can be also triggered by the activation of phospholipase C (PLC), which produces inositol 1,4,5-trisphosphate (IP3) that interacts with Ca^{2+} channels located in the ER and Golgi apparatus (GA), causing their opening. Three IP3 receptor (IP3R) isoforms are expressed in mammals, while a single IP3R is present in Drosophila (itpr) (Yoshikawa et al., 1992). The channel shares the highest level of similarity as well as functional properties (channel 86 conductance, gating properties, IP3- and Ca^{2+}-dependence) with the mouse IP3R1.

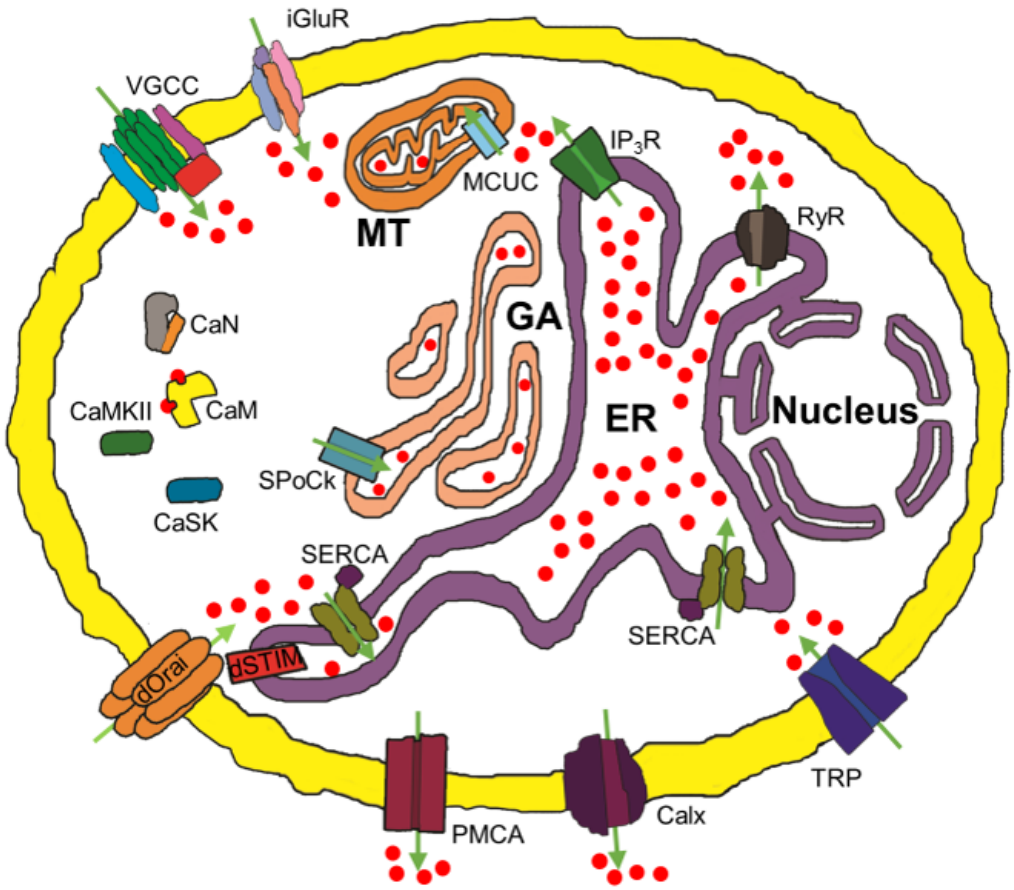

Figure 5. A Drosophila cell with its Ca^{2+}toolkit. The movement of Ca^{2+} ions (red spots) are indicated as green arrows. The Ca^{2+} handling proteins inserted in the PM, from the upper left corner, are: Voltage-Gated Ca^{2+} channels (VGCC), glutamate-gated ionotropic receptors (iGluRs), Transient Receptor Potential (TRP) channels, Na+/Ca^{2+} exchanger (Calx), PM Ca^{2+} ATPase (PMCA) and ORAI1 oligomers forming a channel. In the ER membrane from the upper left side are present: inositol 1,4,5-trisphosphate receptor (IP3R), Ryanodine Receptor (RyR), Sarco-Endoplasmic Reticulum Ca^{2+} ATPase (SERCA) and STIM1. In the GA membrane is present the Secretory Pathway Ca^{2+} ATPase (SPoCk). The inner mitochondrial membrane hosts the mitochondrial calcium uniporter complex (MCUC). Different Ca^{2+} interacting proteins are resident in the cytosol: Calcineurin (CaN), Calmodulin (Cam), Ca^{2+}/Calmodulin-dependent protein kinase II (CaMKII), and Ca^{2+}/Calmodulin-dependent serine protein kinase (CaSK).

The release of Ca^{2+} from intracellular stores occurs also through Ryanodine Receptor (RyR), located in the sarco/endoplasmic reticulum (SER) membrane. In vertebrates, three isoforms are described (RyR 1–3), while the Drosophila genome contains a single RyR gene that encodes a protein with approximately 45% identity with the vertebrate family members (Hasan and Rosbash, 1992; Takeshima et al., 1994). Ca^{2+} release from intracellular stores is most often accompanied by Ca^{2+} influx through PM channels in the regulated process of

SOCE. The molecular basis of SOCE, whereby Ca^{2+} influx across the PM is activated in response to depletion of ER Ca^{2+} stores, has been under investigation for more than 20 years and was finally revealed thanks to the identification of the two molecular key players in RNAi screens performed in Drosophila S2 cells (Roos et al., 2005; Zhang et al., 2006b). The presence of a single fly homologue for stromal interacting molecule 1 (STIM1) and ORAI1, whereas mammals have two and three copies respectively, offered a flying start for the identification of the proteins. The main route for Ca^{2+} uptake into mitochondria is through the mitochondrial calcium uniporter (MCU) complex, a Ca^{2+}-selective ion channel located at the inner mitochondrial membrane. The channel subunit MCU is regulated through other regulatory components, i.e. MICU1/2/3 and EMRE (Pendin et al., 2014). A MCU homologue has been identified and characterized in Drosophila (Drago and Davis, 2016; Walkinshaw et al., 2015), along with its regulatory subunits MICU1 (Drago and Davis, 2016; Walkinshaw et al., 2015) and EMRE (Choi et al., 2017). Ca^{2+} signals are terminated by the combined activities of Ca^{2+} ATPases, located on PM, ER, GA membranes and the Na+/Ca^{2+} exchanger, NCX. PM Ca^{2+} ATPase (PMCA) is a transport protein present in all animals, characterized by a high Ca^{2+} affinity and a low-transport capacity that extrudes Ca^{2+} from the cytosol to maintain [Ca^{2+}] at the basal value of about 100 nM. In humans and other mammals, four major PMCA isoforms are encoded by separate genes, while the Drosophila genome encodes a single, ubiquitously expressed PMCA (Bai et al., 2008). The ATPases located on ER and GA membranes acts to re-accumulate the cation in the organelles' lumen. The SER Ca^{2+} ATPase (SERCA), transports inside ER/SR two Ca^{2+} ions per ATP hydrolyzed. In vertebrates, three SERCA protein isoforms are encoded by three distinct genes, while in Drosophila a single gene was identified (Magyar and Váradi, 1990). Fly SERCA has a higher identity with mammalian SERCA1 and SERCA2 (71–73%) and is expressed at a very high level in the central nervous system (CNS) and muscles. A single homolog of the Secretory Pathway Ca^{2+} ATPase (SPCA) is present in Drosophila, named SPoCk. The gene results in three isoforms, but only one (SPoCk-A) has been reported to localize in GA membranes, as its mammalian counterpart (Southall et al., 2006). The

other two variants have been reported to localize in the ER and peroxisomal membranes. The NCX is a non-ATP-dependent antiporter that mediates the efflux of Ca^{2+} ions in exchange for Na^{2+} import. The Drosophila NCX, named Calx, is highly expressed in brain and muscle and has 55% identity with the three mammalian isoforms NCX1, NCX2 and NCX3, which are differentially expressed mainly in the heart, brain and skeletal muscles, respectively (Schwarz and Benzer, 1997).

Ca^{2+} Indicators for Imaging in Flies

Approximately 30 years ago, scientists started to design and engineer organic fluorescent Ca^{2+} indicators, opening the door for cellular Ca^{2+} imaging. Since then, a variety of probes have been developed, which differ in their mode of action, Ca^{2+} affinities, intrinsic baseline fluorescence and kinetic properties. Two major classes of Ca^{2+} indicators have been developed, i.e., chemical probes and genetically encoded Ca^{2+} indicators (GECIs).

GECIs include different types of engineered proteins, such as single fluorescent protein-based indicators (e.g., GCaMP), bioluminescent probes (e.g., aequorin) and fluorescence (or Förster) resonance energy transfer (FRET)- based indicators (e.g., cameleons) (Pendin et al., 2017).

GCaMP is one of the most used GECIs, based on a circularly-permuted variant of Green Fluorescent Protein (cpGFP). The N-terminus of the cpGFP is connected to the M13 fragment of the myosin light chain kinase, while the C-terminus ends with the Ca^{2+}-binding region of calmodulin (CaM). In the presence of Ca^{2+}, M13 wraps around Ca^{2+}-bound CaM, leading to a conformational change that increases the fluorescence protein (FP) fluorescence intensity (Nakai et al., 2001). During recent years, different variants of GCaMP indicators have been developed, with improved characteristics in terms of Ca^{2+} affinity, brightness, dynamic range. Other variants of FPs, e.g., red-coloured, have been used to develop sensors allowing simultaneous measurement in different organelles, making GCaMPs a whole family of great tools to follow Ca^{2+} dynamics.

One limitation in the use of GCaMPs, and in general of single protein based GECIs, is the sensitivity to movement artifacts as well as focal plane shifts, which can be mistaken for [Ca^{2+}] changes. A method used to correct for this type of artifacts is to co-express a FP together with the GECI (Berry et al., 2015).

Alternatively, the limit can be overcome by using ratiometric indicators, such as cameleon. This molecule uses the same Ca^{2+} binding domains of the GCaMP (M13 and CaM), that are bound to two different variants of the GFP: a cyan (CFP) and a yellow (YFP) variant. In the absence of Ca^{2+}, the excited CFP emits at 480 nm, while in the presence of Ca^{2+} the interaction between Ca^{2+}, CaM and M13 brings the two FPs at a closer distance (2–6 nm), and the energy released from the CFP is absorbed by the YFP, that emits at a different wavelength (535 nm). By calculating the ratio of EYFP/ECFP emissions, one obtains a clear indication of intracellular [Ca^{2+}] variations, excluding changes of fluorescence caused by artefactual movements of the sample. GECIs allow the monitoring of Ca^{2+} not only in the cytosol, but also in organelles (e.g., ER, mitochondria, GA, etc.) thanks to the addition of specific targeting sequences. GECIs have demonstrated valuable in the measurement of [Ca^{2+}] in cells and within organelles in several in vivo models. Notably, in flies, the ease of transgenesis allowed the generation of several lines for the expression of GECIs, both cytosolic and organelle-targeted. Moreover, the Gal4-UAS expression system (Brand and Perrimon, 1993; Klueg et al., 2002) allows the targeting of the probes to specific tissues or even cell subtypes. In this two-part approach, one fly strain carries the Ca^{2+} sensor cDNA under the control of an upstream activator sequence (UAS), so that the gene is silent in the absence of the transcription factor Gal4. A second fly strain expressing Gal4 in a cell type-specific manner is mated to the UAS strain, resulting in progeny expressing the probe in a transcriptional pattern that reflects the expression pattern of the Gal4 line promoter.

Chemical indicators (e.g., quin-2, fura-2, indo-1, fluo-4) (Grynkiewicz et al., 1985; Tsien, 1980; Tsien et al., 1982) are small fluorescent molecules that are able to chelate Ca^{2+} ions. These molecules are based on BAPTA, an EGTA homologue with high selectivity for Ca^{2+}. The Ca^{2+} chelating carboxyl groups are usually

masked as acetoxymethyl esters, making the molecule more lipophilic and allowing an easy entrance into cells. Once the molecule is inside the cell, the Ca^{2+} binding domains are freed by cellular esterases (Rudolf et al., 2003). Binding of a Ca^{2+} ion to the molecule leads to either an increase in quantum yield of fluorescence or an emission/excitation wavelength shift. Fura-2 has two excitation wavelengths, 340 and 380 nm, and it emits at 510 nm. When the dye is excited at 340 nm, the fluorescence at 510 nm increases upon Ca^{2+} binding, while it decreases when the excitation is at 380 nm. Thus, by alternatively exciting the dye at 340 and 380 nm and by collecting the emission at 510 nm, one can calculate the ratio between the fluorescence emitted (F_{340}/F_{380}).

The ratiometric nature of fura-2 allows to overcome possible issues due to focal planes shift. Moreover, the probe can be easily loaded in primary cultures, which are sometimes difficult to transfect with GECIs.

Drosophila: Models of Neurodegenerative Diseases

Changes in intracellular [Ca^{2+}] mediate a wide range of cellular processes that are relevant to neurodegenerative disorder etiology, including learning and memory, as well as cell death (Giorgi et al., 2018). Indeed, a close link between the pathogenesis of different neurodegenerative disorders and Ca^{2+} regulating systems, the so called "Ca^{2+} hypothesis of neurodegenerative diseases", has been convincingly corroborated by several experimental findings (Mattson, 2004, 2007). The potential of the approaches described above makes flies a powerful model system to elucidate pathogenic processes in neurobiology. Indeed, a wide collection of fly models of neurodegenerative disorders have been developed. Often, the model consists of targeted expression of human disease-associated protein. In the case of loss of function pathologic mutations, also knock out/knock down approaches have proved successful in mimicking the pathology. In many cases, robust neurodegeneration is observed in these models. Ca^{2+} imaging experiments performed in fly models of neurodegenerative dis- orders have helped unravel the pathogenesis of diseases, including Alzheimer's disease (AD), Parkinson's Disease (PD), Huntington Disease (HD). AD is a

neurodegenerative disorder characterized by deposition of amyloid β (Aβ) in extracellular neuritic plaques, formation of intracellular neurofibrillary tangles and neuronal cell death. Among familial (FAD) cases, approximately 50% have been attributed to mutations in three genes: amyloid β precursor protein (APP) (Goate et al., 1991), Presenilin 1 (PSEN1) (Sherrington et al., 1995) and presenilin 2 (PSEN2) (Rogaev et al., 1995). The fly genome encodes a single Presenilin gene (Psn) (Boulianne et al., 1997) and a single APP orthologue (Appl) which encodes for β-amyloid precursor-like protein. Drosophila models of AD have been developed, mostly expressing WT and FAD-mutant forms of human APP and presenilins, reproducing AD phenotypes, such as Aβ deposition, progressive learning defects, extensive neurodegeneration and ultimately a shortened lifespan (Iijima et al., 2004). It is now accepted that FAD-linked presenilins mutants are responsible for a dysregulation of cellular Ca^{2+} homeostasis. An imbalance of Ca^{2+} homeostasis is supposed to represent an early event in the pathogenesis of FAD, but the mechanisms through which FAD-linked mutants affect Ca^{2+} homeostasis are controversial (Agostini and Fasolato, 2016). Using a fly model of FAD, Michno and colleagues (Michno et al., 2009), showed that expression of WT or FAD-mutant Psn in Drosophila cholinergic neurons results in cell-autonomous deficits in Ca^{2+} stores, highlighted using the chemical Ca^{2+} probe fura-2. Importantly, these deficits occur independently of Aβ generation. They also describe a novel genetic, physiological and physical interaction between Psn and Calmodulin, a key regulator of intracellular Ca^{2+} homeostasis. More recently, a study conducted by Li et al. (Li et al., 2018) exploited Ca^{2+} probes and confocal imaging to demonstrate that Imidazole, by decreasing the level of intracellular Ca^{2+}, can rescue the mental defect in Aβ42-expressing flies. PD is the most common movement disorder, typically affecting people between 50 and 60 years of age. The disease is mostly sporadic, only a small fraction of PD cases has been linked to mutations in specific genes, including a-synuclein (Polymeropoulos et al., 1997), parkin (Kitada et al., 1998), PINK1 (Valente et al., 2004). Cytoplasmic aggregates mainly formed by α-synuclein protein, called Lewy bodies (Spillantini et al., 1997), are usually found in the substantia nigra of brain tissue. Dopaminergic neurons are the most susceptible to degeneration in

PD. Fruit flies are largely used as model for PD. Expression of human α-synuclein in flies leads to selective loss of dopaminergic neurons in the adult brain over time and accumulation of protein in cytoplasmic inclusions (Feany and Bender, 2000). Pan-neural expression of α-synuclein either WT or carrying PD-linked mutations results in premature loss of climbing ability. Noteworthy, the first animal models revealing an interaction between the two PD genes homologues Pink1 and parkin have been developed in Drosophila (Clark et al., 2006; Park et al., 2006). Recently, Ca^{2+}-induced neurotoxicity have been explored in a Drosophila model of retinal degeneration. The authors found that increasing the autophagic flux prevented cell death in mutant flies, and this depended on the Pink1/parkin pathway (Huang et al., 2016). HD is a progressive brain disorder characterized by uncontrolled movements, emotional problems, and loss of cognition. The disease is caused by autosomal dominant mutations in the gene encoding for huntingtin (HTT), resulting in an abnormal expansion of the number of CAG triplets, encoding for Glutamine. A Drosophila model of HD have helped investigating the mechanisms by which expanded full-length huntingtin (htt) impairs synaptic transmission (Romero et al., 2008). The authors showed that expression of expanded full-length htt led to increased neurotransmitter release and increased resting intracellular Ca^{2+} levels, compared to controls. Moreover, mutations in voltage-gated Ca^{2+} channels (VGCCs) restored the elevated [Ca^{2+}] and improved neurotransmitter release efficiency, as well as neurodegenerative phenotypes. This suggests that a defect in Ca^{2+} homeostasis contributes to the pathogenesis of the disease, which is in agreement with observations in mammalian systems (Bezprozvanny and Hayden, 2004; Cepeda et al., 2001; Hodgson et al., 1999; Tang et al., 2005). Drosophila models have been created recapitulating many other diseases affecting the neuronal system, e.g. HSPs. Available tools for Ca^{2+} imaging applied to these models would provide valuable insights in the role of Ca^{2+} in the pathogenesis of neurodegenerative diseases.

Aim of the work

The aim of this work is to uncover a potential correlation between ER shape and function, in particular the organelle's role in maintaining Ca^{2+} homeostasis. This link is investigated in neurons, highly specialized cells that requires a tight control of Ca^{2+} homeostasis. We exploited the fruit fly *Drosophila melanogaster*, as a model organism, taking advantage of its lack of genetic redundancy and ease of handling. ER shape in fly neurons was altered in two different ways: directly, downregulating an ER shaping protein or indirectly, by affecting MT cytoskeleton structure. Indeed, MT organization is supposed to play a role in the regulation of ER distribution and sheet/tubule balance.

Both approaches rely on morphological alterations induced by the manipulation of proteins whose mutation is causative for the neurodegenerative disorder HSP. In particular, MT stability was altered by expressing in flies the MT-severing protein spastin carrying the dominant-negative mutation K467R. Indeed, when $spastin^{K467R}$ is expressed in a WT background, hyper-stabilization of MTs has been observed. To impact directly on ER shape, we downregulated Rtnl1, the fly member of Reticulon protein family which are responsible for ER tubulation. Loss of Rtnl1 leads to an imbalance of ER sheet/tubule ratio, favouring ER sheets at the expenses of tubules.

In the two models described, ER morphology was assessed. Then, Ca^{2+} homeostasis was evaluated on neuronal preparations. In particular, the process of SOCE, strongly dependent on ER dynamics and Ca^{2+} content, was evaluated in depth.

Results

Neuronal expression of spastin^{K467R} affects fly viability and locomotor activity

In order to alter MT stability, a transgenic line, previously generated (Orso et al., 2005), for the expression of Drosophila spastin carrying the mutation K467R under the control of UAS promoter (UAS-Dspastin-K467R) was used. The substitution, located in the AAA ATPase domain, corresponds to the HSP pathogenic mutation K388R in the human spastin protein and it is known to produce a dominant-negative effect (Orso et al., 2005). Indeed, when spastin^{K467R} is expressed in a WT background, hyper-stabilization of MTs has been observed, similar to that produced by the downregulation of spastin (Orso et al., 2005).

The UAS-Gal4 binary system was exploited to drive the expression of spastin^{K467R} in a spatially regulated manner. By crossing the UAS line with a specific strand expressing the Gal4 protein under the control of a pan-neuronal promoter (elav-Gal4), selective expression of spastin^{K467R} in neurons was obtained.

The birth rate and the lifespan of flies expressing spastin^{K467R} in neurons was evaluated. The rate of eclosed individuals carrying mutated spastin was estimated and compared to the rate expected by the mendelian inheritance. The rate of eclosed spastin^{K467R} flies was partially reduced (83% of expected), compared to controls (100% of expected) (Figure 6A). Lifespan of spastin^{K467R} expressing flies was also evaluated: flies were separated in small populations of 15-20 individuals and their survival monitored during ageing. A significant decrease in viability during ageing was observed in flies expressing spastin^{K467R}, compared to controls (Figure 6B). The locomotor capacity of the flies was then evaluated. The most used locomotor assay for Drosophila is the climbing assay, which tests the ability of flies to climb a steep wall. 15-20 flies were placed inside a cylinder and the number of flies that can climb, passing a pre-determined mark

in a certain time window was counted for each genotype. In agreement with previous observations (Orso et al., 2005), spastin^{K467R} expressing flies displayed faster decline in negative geotaxis during ageing, when compared to controls (Figure 6C). These results show that the expression of spastin^{K467R} in neurons impairs fly viability and locomotor activity.

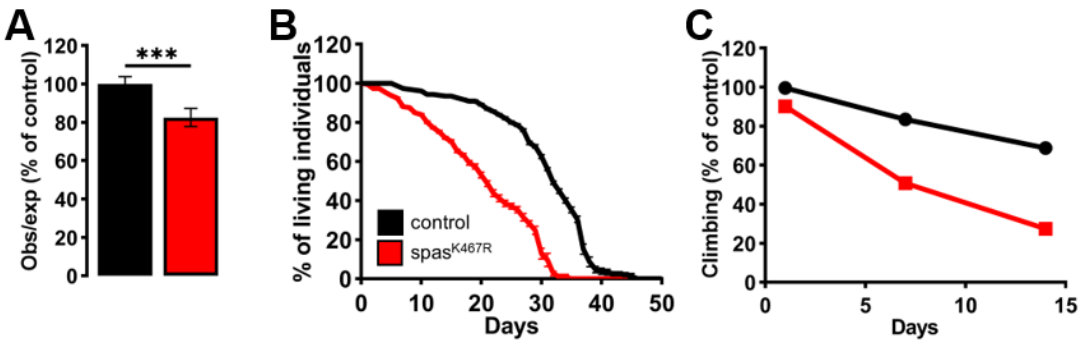

Figure 6. (A) Flies of the two genotypes (Control, black; red, spastin^{K467R}) were counted at the eclosure to define their birth rate. Data are presented as observed/expected flies' ratio. *** $p < 0.001$. **(B)** Evaluation of fly survival: flies were separated in tubes (20 individuals/each) and counted every 2 days during ageing. Data represented as percentage of living flies over 40 days. **(C)** Evaluation of fly climbing ability: flies were tapped at the bottom of a graduated tube. Flies able to cross a 10 cm mark in 60 s were counted as climbing flies. Data shown as percentage of flies able to cross the line at day 1, 7 and 14.

Neuronal expression of spastin^{K467R} influences ER morphology

Despite MTs are implicated in the regulation of ER distribution and sheet/tubule balance (Lu et al., 2009; Terasaki et al., 1986), no information is present in the literature regarding potential ER morphology alterations due to the expression of spastin^{K467R}. We thus examined ER morphology in fly neurons expressing spastin^{K467R}. To visualize the ER structure, we co-expressed the ER luminal marker BiP–sfGFP–HDEL (Summerville et al., 2016), under the control of the motoneuron-specific promoter D42-Gal4. In control motor neuron cell bodies, the ER appears mostly as a network of interconnected tubules. In motor neurons expressing spastin^{K467R}, ER morphology was markedly changed and extended fluorescent areas were often present (Figure 7A). These structures likely

represent ER sheets; however, the resolution of confocal images does not allow the precise discrimination between sheets or tubules. EM represents a valid imaging alternative, since it extraordinarily enhances the resolution of ER morphology, although at the expenses of the three-dimensional structure. By combining light microscopy, TEM and electron tomography it has been previously shown that the length of ER profiles measured on TEM thin sections correlates with tubules/sheets balance (Puhka et al., 2007, 2012). In particular, the conversion of tubules in sheets results in an increase in the length of ER profiles. This allows a clear discrimination between sheets and tubules, based on the length of TEM ER profiles. For this reason, TEM images were taken from thin slices of larval brain neurons expressing spastin^{K467R} (Figure 7B). Analysis of ER profiles revealed, indeed, an increase in their length in spastin^{K467R}-expressing neurons, compatible with an augmented ER sheets amount (Puhka et al., 2012) (Figure 7C). The histogram representing the distribution of ER profiles length (Figure 7D) highlights that the increase of long profiles in spastin^{K467R} expressing neurons is accompanied by a decrease of shorter ER profiles. Together, these observations illustrate that spastin^{K467R} expression causes a sheet/tubule imbalance, with an enrichment of ER sheet at the expenses of tubules.

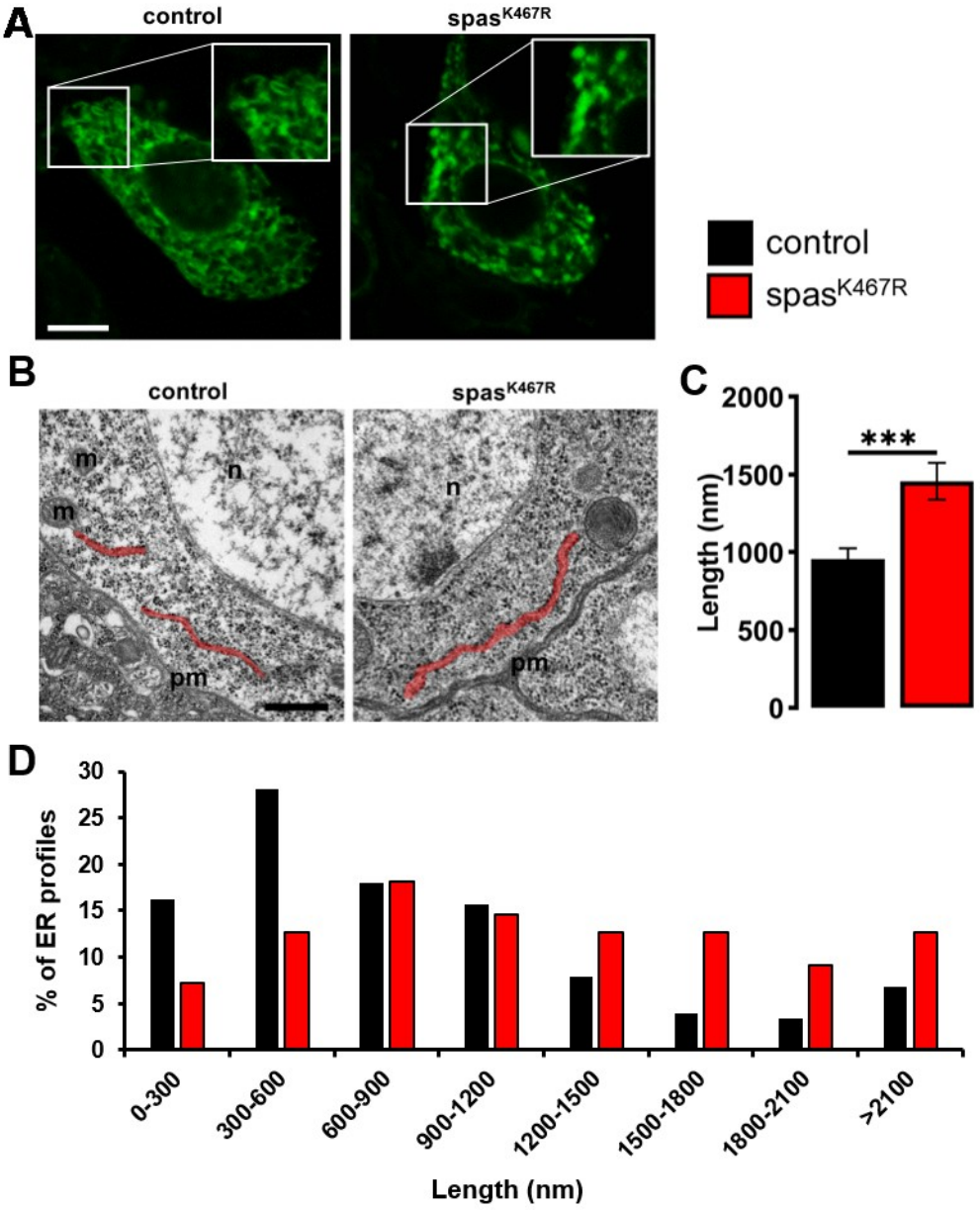

Figure 7. (A) Confocal images of ventral ganglion motor neuron cell bodies of larvae of the indicated genotypes co-expressing BiP-sf-GFP-ER. Scale bar, 50 µm. **(B)** Transmission electron microscopy (TEM) images of ventral ganglion neuronal cell bodies of larvae expressing spastin^{K467R} and relative control; ER profiles are highlighted in red. pm, plasma membrane; n, nucleus; m, mitochondria. Scale bar, 500 nm. **(C)** Quantification of ER profiles' mean length in the indicated genotypes. Mean ± SEM, N ≥ 50. *** $p < 0.001$. **(D)** Distribution of ER profiles length measured in TEM images of ventral ganglion neuronal cell bodies of larvae expressing spastin^{K467R} (red) and relative controls (black). For each class (in nm) the relative abundance (percentage of total profiles number) is displayed. N ≥ 50 profiles.

Axons are believed to contain primarily smooth ER tubules that tracks to axon termini (Krijnse-Locker et al., 1995; S. Tsukita, 1976; Terasaki, 2018; Terasaki and Reese, 1994). Consistently with the decrease in ER tubules observed in cell bodies, in larvae expressing spastin^{K467R}, distal axons appear devoid of ER (Figure 8). Although it cannot be excluded that this phenotype is due to a general organelle trafficking impairment due to spastin^{K467R}-induced hyper-stabilization of axonal MTs, this result is compatible with a general reduction of ER tubules. Altogether, these results indicate that the expression of the dominant-negative spastin mutant strongly alter physiological ER morphology, causing an enrichment of ER sheets to the detriment of tubules.

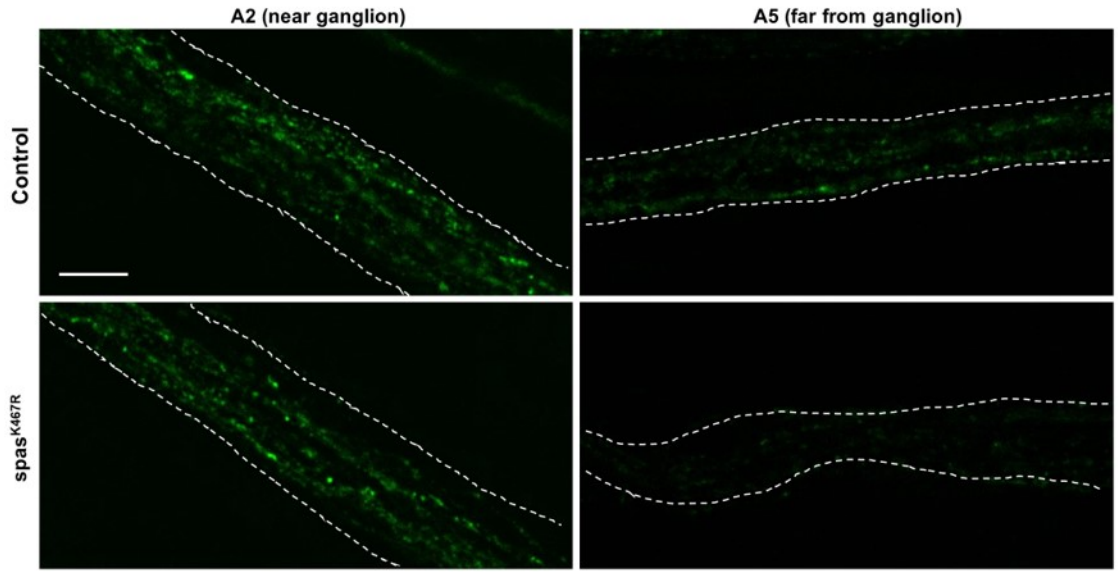

Figure 8. Confocal images of motor neuron nerves of larvae of the indicated genotypes co-expressing BiP-sf-GFP-ER. Pictures on the left were acquired at the level of A2 larval segment, *i.e.,* near the cell bodies, while pictures on the right were acquired at the level of larval segment A5, *i.e.,* far from the cell bodies. Scale bar, 50 µm.

Neuronal expression of spastin^{K467R} affects ER Ca^{2+} handling

The observed morphological alteration likely impact on definite ER functions that depend very much on the presence of tubular ER. Specifically, the movement of

ER tubules through the TAC-mediated mechanism is believed to be directly involved in the activation of SOCE, the process necessary to replenish empty ER Ca^{2+} stores. To investigate the impact of spastin^{K467R} expression on ER Ca^{2+} dynamics, and specifically on SOCE, we exploited neuronal preparation from fly brains. Neurons were isolated from brains of larvae expressing spastin^{K467R} under the control of a pan-neuronal promoter (elav-Gal4/UAS-spastin^{K467R}) or from controls (elav-Gal4/+). Isolated neurons were maintained in culture for 16-18 hours (Chakraborty and Hasan, 2018) and then loaded with the cytosolic Ca^{2+} indicator fura-2 and examined by fluorescence microscopy. Before imaging experiments, the health of neuronal preparation was verified by assessing neuronal morphology. Neurons looked healthy and neuronal processes were often visible (Figure 9A). The typical protocol to visualize SOCE comprehend the depletion of intracellular Ca^{2+} stores in a Ca^{2+}-free medium and the subsequent Ca^{2+} re-addition. Stores were depleted by cell treatment with the SERCA inhibitor thapsigargin in a Ca^{2+}-free medium. By inhibiting the SERCA pump, the ER Ca^{2+}-uptake mechanism is inhibited, promoting the passive leak of Ca^{2+} towards the cytoplasm. The increase in $[Ca^{2+}]_c$ is balanced by the activity of the PMCA that actively extrudes Ca^{2+} extracellularly in order to maintain its cell homeostasis, leading to a progressive and complete depletion of ER Ca^{2+} content. Thapsigargin was applied to neurons for 10 minutes, in order to completely deplete the ER. Ca^{2+} depletion allows dStim-dOrai complex to form and the oligomerization of dOrai, thus forming the PM-located CRAC channel. SOCE was then monitored at the fluorescence microscope upon $CaCl_2$ addition (Ca^{2+}, 2 mM). A large $[Ca^{2+}]_c$ increase, followed by a sustained plateau, due to Ca^{2+} influx across the PM, was observed in control neurons (Figure 9B). The effect of spastin^{K467R} on SOCE was quantified by calculating the area under the curve, corresponding to the first two minutes of Ca^{2+} influx. A marked decrease in SOCE was observed in neurons from larvae expressing spastin^{K467R}, compared to controls (37% reduction, $p < 0.001$; n = 350 control cells; n = 300 spastin^{K467R} cells; Figure 9C).

It is known that differences in PM potential alter the driving force for Ca^{2+} entry, thus potentially affecting the extent of SOCE (Penner et al., 1993). To nullify

possible differences in PM potential between the two genotypes, SOCE was measured following the protocol described above but in a medium where NaCl was iso-osmotically substituted by K-D-gluconate (K^+-based medium, see Materials and Methods for details). Bathed in this latter medium, cells are completely depolarized, abolishing possible differences in PM potential between the two genotypes. A higher concentration of $CaCl_2$ (5 mM) was re-added in this latter case, to obtain an appreciable Ca^{2+} influx, after emptying the stores, in a condition with reduced electrical gradient. The effect of spastin^{K467R} expression on SOCE was however similar to that found in the standard Na^+-containing medium (38% reduction, $p < 0.001$; n = 300 control cells; n = 280 spastin^{K467R} cells) (Figure 9D-E).

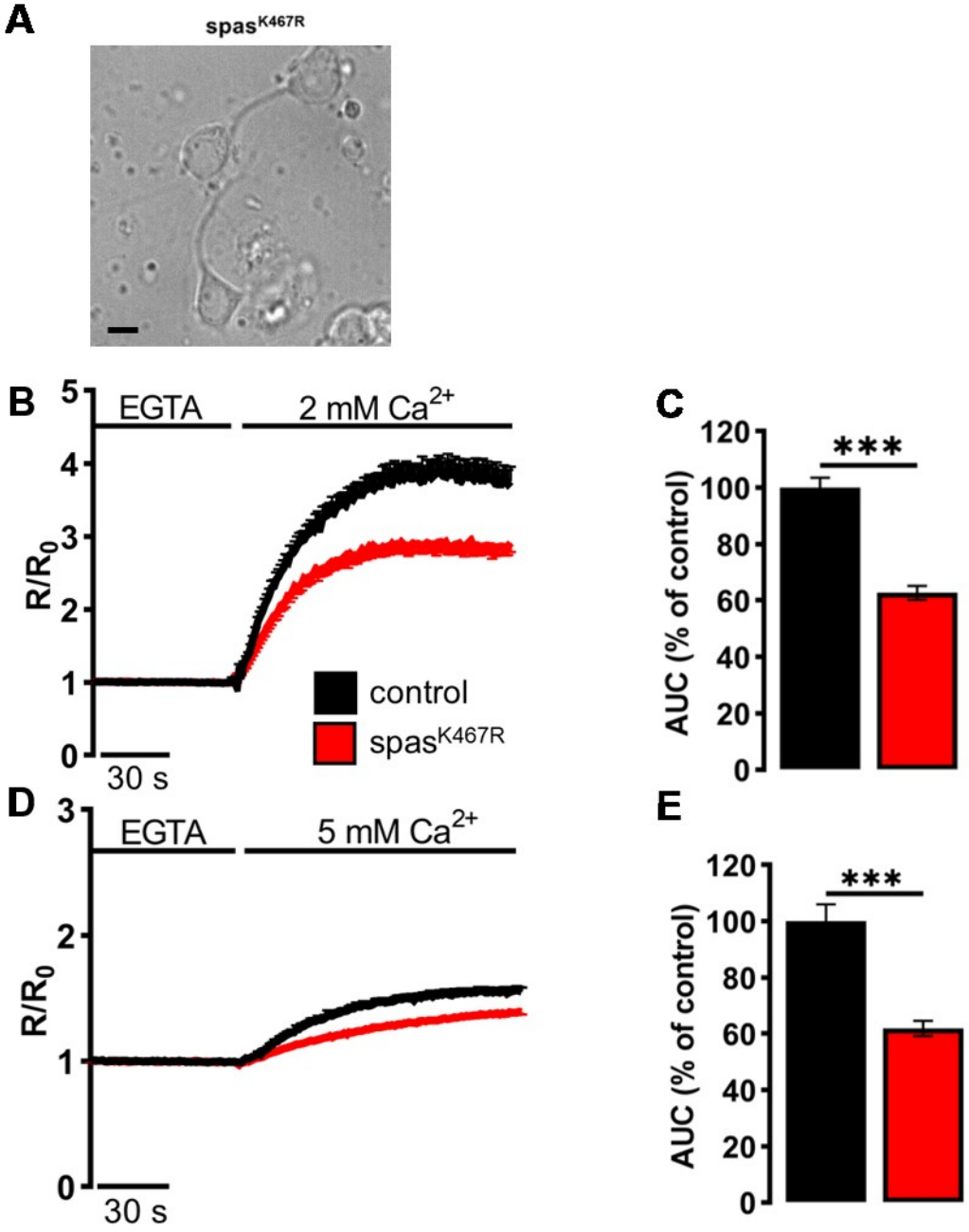

Figure 9. (A) A bright field image of neurons dissociated from larval brains expressing spastin^{K467R}. Scale bar, 50 μm. **(B, D)** Cytosolic Ca^{2+} dynamics induced by SOCE activation in neurons dissociated from larval brains expressing spastin^{K467R}, and relative controls, as detected by fura-2. Cells were pre-treated with thapsigargin in a Ca^{2+}-free medium for 10 min, to empty intracellular Ca^{2+} stores, and then **(B)** 2 mM or **(D)** 5 mM $CaCl_2$ was added. In all panels, average traces are represented as R/R_0 of N > 100 cells. **(C, E)** Histograms report the average area under curve (AUC) of the traces recorded. Data are presented as mean ± SEM of N > 100 cells. *** $p < 0.001$.

To exclude that the difference in $[Ca^{2+}]_c$ increases measured in the two genotypes upon Ca^{2+} re-addition was due to unspecific PM Ca^{2+} leaks or other Ca^{2+} influxes, basal Ca^{2+} entry was measured in the same cells, by simply adding back Ca^{2+} to cells bathed in a Ca^{2+}-free medium, without emptying intracellular stores. No differences were found between the two genotypes, neither in standard medium nor in K^+-based medium (Figure 10A-D).

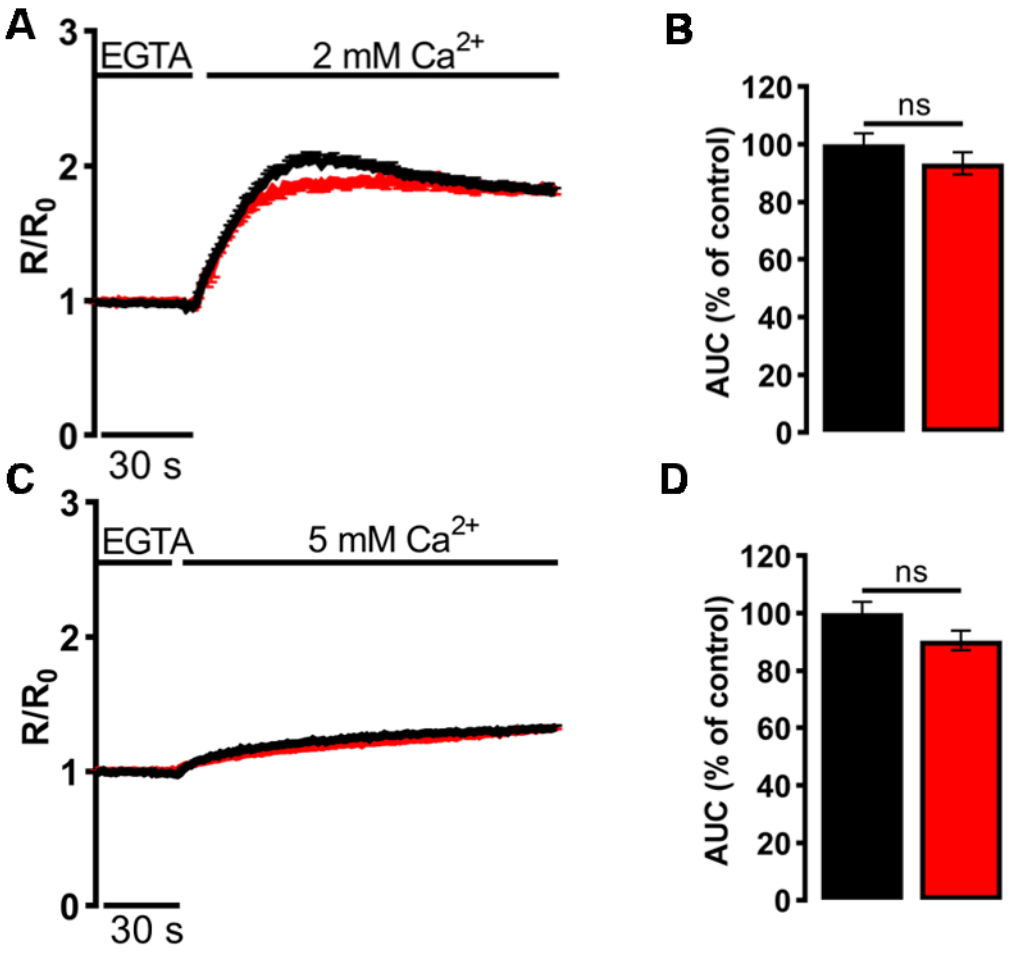

Figure 10. Cytosolic Ca^{2+} dynamics induced by Ca^{2+} re-addition in standard medium **(A)** or in K^+-based medium (see Materials and Methods) **(C)** in neurons dissociated from larval brains expressing spastin^{K467R}, and relative controls, as detected by fura-2. Cells were kept in EGTA for 30 s and then **(A)** 2 mM or **(C)** 5 mM $CaCl_2$ was added. Traces are presented as average R/R_0 values of N > 200 cells. **(B, D)** Histograms reporting the average area under curve (AUC) of the traces. Data are presented as mean ± SEM of N > 100 cells. *** $p < 0.001$

The decrease in SOCE could cause a partial depletion of intracellular Ca^{2+} stores in spastin^{K467R} expressing neurons. To investigate this possibility, neurons were

loaded with fura-2 and the Ca^{2+} ionophore ionomycin was applied to neurons bathed in a Ca^{2+}-free medium containing the Ca^{2+} chelator EGTA. In this condition, the observed $[Ca^{2+}]_c$ rise is due to the discharge of all non-acidic intracellular Ca^{2+} stores (Figure 11A). The increase in $[Ca^{2+}]_c$ elicited by ionomycin was significantly reduced in spastin^{K467R} expressing neurons, relative to controls, as indicated by the area under the curve obtained upon ionomycin addition (22% reduction, $p < 0.001$; n = 90 control cells; n = 100 spastin^{K467R} cells; Figure 11B). Since ionomycin discharge only non-acidic compartments, monensin was subsequently added, in order to dissipate pH gradients in intracellular membranes and discharge any residual Ca^{2+} present in acidic pools (Fasolato et al., 1991); this addition however did not result in an appreciable $[Ca^{2+}]_c$ increase in neither genotypes (data not shown), indicating the relatively low abundance of this type of Ca^{2+} store in these cells. The results indicate that the Ca^{2+} content of intracellular stores is diminished in cells expressing spastin^{K467R} mutation. To determine whether the observed reduction was due to a specific partial depletion of the ER Ca^{2+} store, dissociated neurons were treated with the SERCA inhibitor CPA, thus inducing the passive release of Ca^{2+} from the organelle, resulting in a transient increase in $[Ca^{2+}]_c$. The amplitude of the increase in $[Ca^{2+}]_c$ is a reflection of the Ca^{2+} content derived only from the ER and the cis/medial-Golgi, the main intracellular Ca^{2+} stores equipped with SERCA pumps (Pizzo et al., 2010). The increase in $[Ca^{2+}]_c$ elicited by CPA was significantly reduced in spastin^{K467R} expressing neurons, relative to controls (Figure 11C). The extent of such reduction, estimated calculating the area under the curve above resting $[Ca^{2+}]_c$ values, was 28% ($p < 0.001$; n = 220 control cells; n = 160 spastin^{K467R} cells; Figure 11D). Thus, ER Ca^{2+} content is diminished in cells expressing spastin^{K467R}. After CPA application, the discharge of residual pools, by ionomycin addition, did not show any difference between control and spastin^{K467R}-expressing neurons (Figure 11E-F), indicating that spastin mutation primarily affects $[Ca^{2+}]_{ER}$.

Altogether, these results indicate that expression of spastin^{K467R} causes an impairment of the ER Ca^{2+} replenishment mechanism of SOCE. This likely results in a reduction of the steady-state $[Ca^{2+}]_{ER}$.

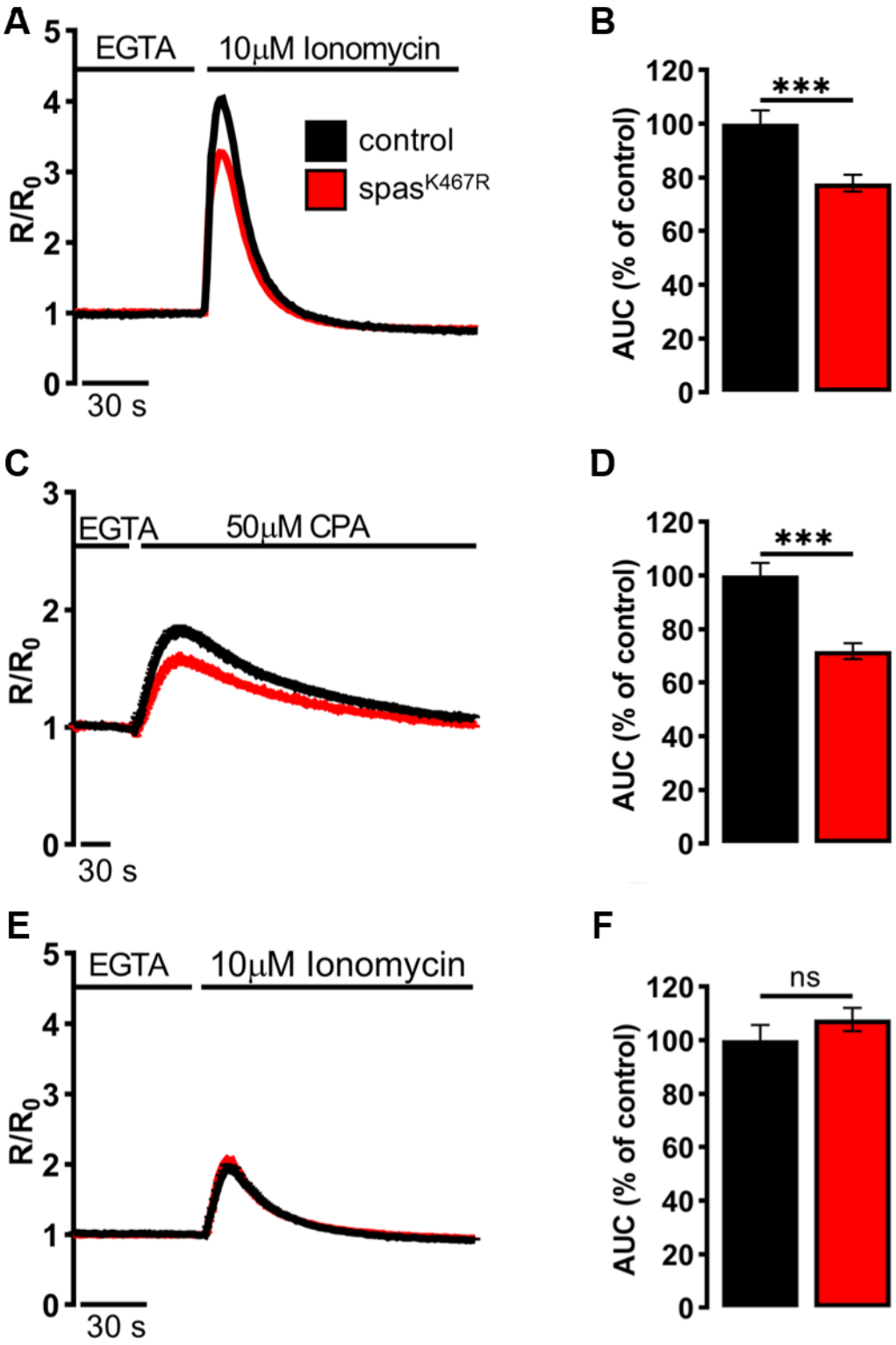

Figure11. Cytosolic Ca^{2+} dynamics induced by **(A, B)** ionomycin, **(C, D)** CPA **(E, F)** ionomycin after CPA (as described in **(C))** in neurons dissociated from larval brains expressing spastin^{K467R}, and relative controls, detected by fura-2. **(A, C, E)** Cells were stimulated with **(A, E)** 10 μM ionomycin or **(C)** 50 μM CPA, in a Ca^{2+}-free medium and in the presence of the

Ca^{2+} chelator EGTA. In all panels, average traces are represented as R/R_0 of N > 100 cells. **(B, D, F)** Histograms report the average area under curve (AUC) of the traces recorded. Data are presented as mean ± SEM of N > 100 cells. *** $p < 0.001$.

Vinblastine treatment rescues ER morphology and Ca^{2+} handling defects induced by spastin^{K467R} expression

In order to prove whether MT cytoskeleton impairment was the earliest responsible for ER morphology and Ca^{2+} handling defects observed in spastin^{K467R}-expressing flies, and to exclude other possible effects of mutant spastin expression, a pharmacological approach was exploited. It has been shown that administration of low concentrations of the MT-depolymerizing drug vinblastine rescued the excessive stabilization of MTs in spastin^{K467R}-expressing flies (Orso et al., 2005). Vinblastine was thus administered to control and spastin^{K467R} flies by addition to the food at a concentration of 50 nM (Orso et al., 2005). The ER morphology of treated larvae co-expressing the ER marker BiP–sfGFP–HDEL (Summerville et al., 2016) was then examined in neurons by confocal imaging. Image analysis indicated that the exposure to the MT-targeting drug results in the recovery of ER morphology in flies expressing spastin^{K467R} (Figure 12A, compare to Figure 7A). Again, TEM images were taken from thin brain slices of larvae expressing spastin^{K467R} and treated with vinblastine. Analysis of neuronal images from these slices showed that vinblastine treatment causes a decrease in the length of ER profiles, compared to untreated spastin^{K467R}-expressing neurons (Figure 12B-C). Accordingly, the distribution of the ER profiles' length resembles that of control flies (Figure 12D). These results indicate that vinblastine-induced destabilization of MTs recovers the sheet/tubules imbalance caused by spastin^{K467R} expression.

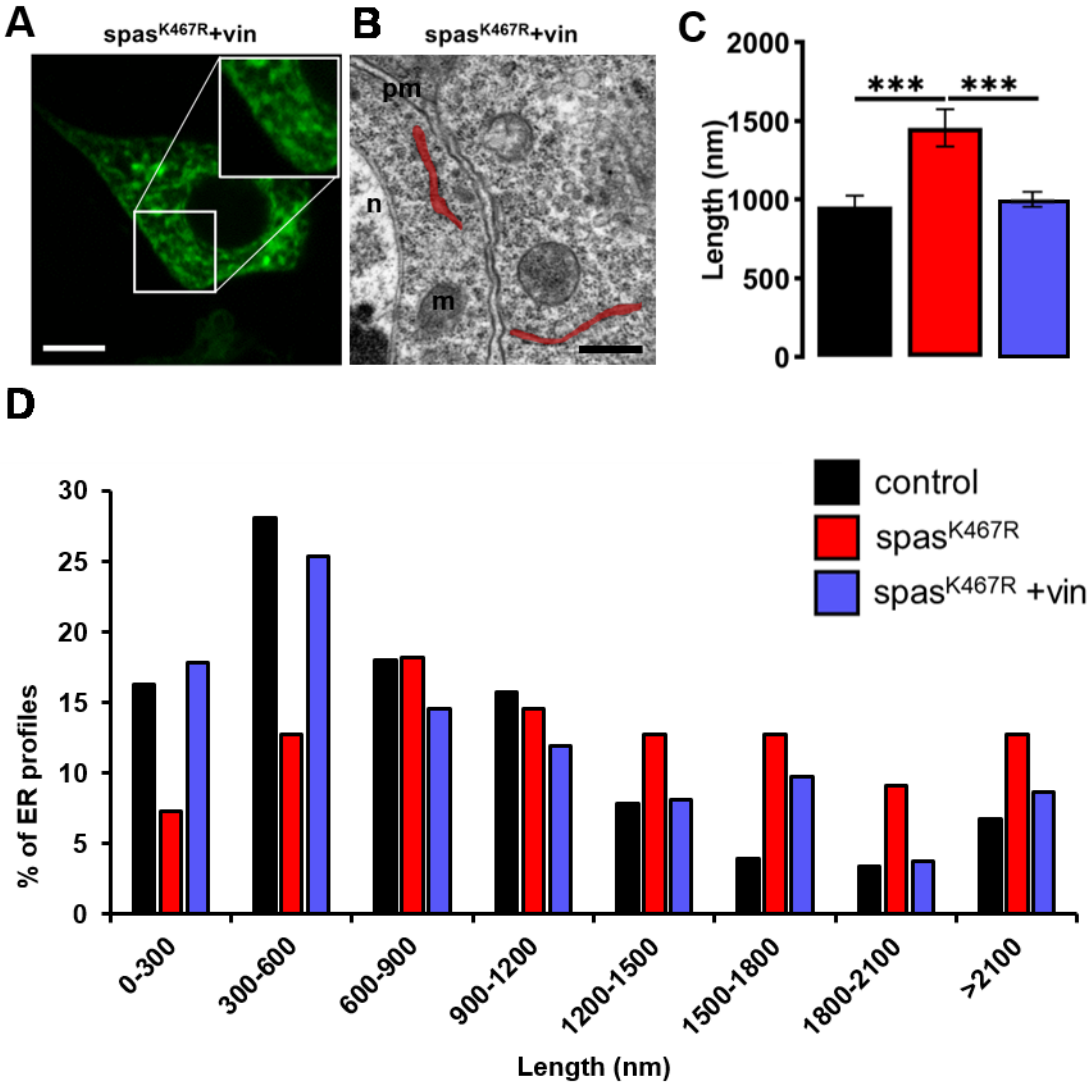

Figure 12. (A) Confocal image of a ventral ganglion motor neuron cell body of a larva co-expressing BiP-sf-GFP-ER and spastin^{K467R} raised in vinblastine-containing food (50 nM). Compare this image to that in Figure 1A. Scale bar, 50 µm. **(B)** Transmission electron microscopy (TEM) image of ventral ganglion neuronal cell bodies of a larva expressing spastin^{K467R} treated with vinblastine; ER profiles are highlighted in red. pm, plasma membrane; n, nucleus; m, mitochondria. Compare the image to that in Figure 1B. Scale bar, 500 nm. **(C)** Quantification of ER profiles' mean length for the indicated genotypes, with or without vinblastine treatment. Mean ± SEM, N ≥ 50. *** $p < 0.001$. **(D)** Distribution of ER profiles length measured in TEM images of ventral ganglion neuronal cell bodies of larvae of the indicated genotype, with or without vinblastine treatment. For each class (in nm) the relative abundance (percentage of total profiles number) is displayed. N ≥ 50 profiles.

Moreover, in neurons dissociated from brains of the same larvae, SOCE was evaluated as described above. After the treatment with vinblastine, the reduction in the Ca^{2+} entry following stores depletion, observed in neurons derived from larvae expressing spastin^{K467R}, was partially recovered (Figure 13A-B), indicating that the drug-induced destabilization of hyper-stabilized MTs rescues the spastin^{K467R}-induced SOCE defects.

It has been shown that loss of MT polymers in response to vinblastine occurs very rapidly, starting in as little as 30 minutes (Harkcom et al., 2014). In order to further demonstrate that the rescue of MT cytoskeleton is directly responsible for the recovery of SOCE impairment observed in spastin^{K467R} expressing flies, the treatment with vinblastine (1 μM) was performed also acutely on dissociated neurons from spastin^{K467R} larvae raised in the absence of the drug. Application of vinblastine for 50 minutes before SOCE analysis was able to induce a partial rescue in the extent of Ca^{2+} entry, when compared to that of untreated spastin^{K467R}-expressing neurons (Figure 13C-D). This result indicates that the re-establishment of proper MT organization is sufficient to rescue the process of Ca^{2+} entry upon stores depletion, affected by the spastin mutant.

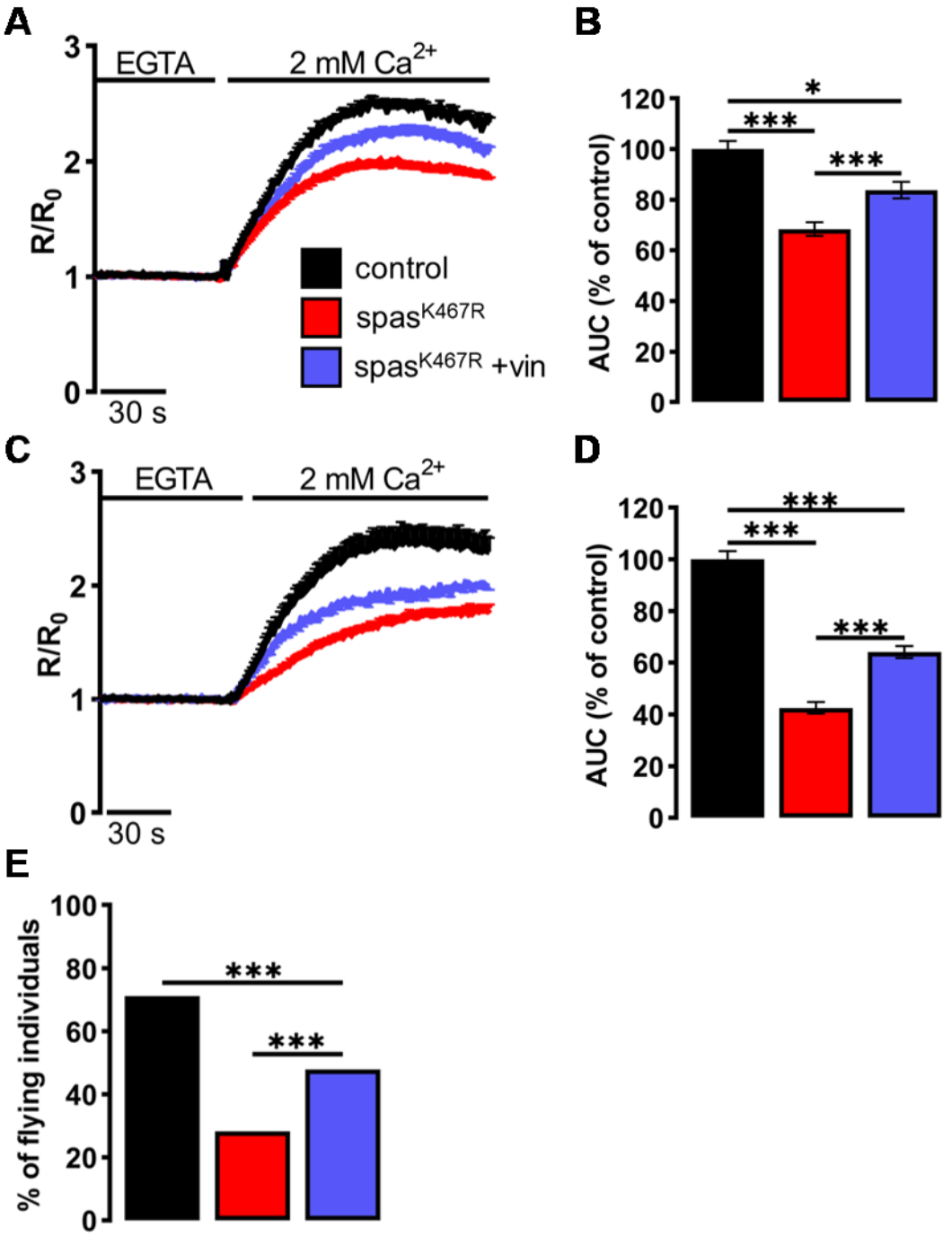

Figure 13. (A-D) Cytosolic Ca^{2+} dynamics induced by SOCE activation in neurons dissociated from larval brains expressing spastin^{K467R}, and relative controls, as detected by fura-2. Where indicated, vinblastine was applied: **(A, B)** before dissociation, larvae were chronically treated with 50 nm vinblastine; **(C, D)** after dissociation, neurons were acutely treated with 1 μM vinblastine. Cells were pre-treated with thapsigargin for 10 min to empty intracellular Ca^{2+} stores, then, 2 mM $CaCl_2$ was added. Traces are presented as average R/R_0 values of N > 100 cells. **(B, D)** Histograms reporting the average area under curve of the corresponding traces. Data are presented as mean ± SEM of N > 100 cells. * < 0.05; *** < 0.001. **(E)** Flight ability, assayed by the cylinder drop test, of animals expressing spastin^{K467R} and relative controls. Where

indicated, animals were chronically exposed to vinblastine (50 nM). Data are presented as the percentage of flying individuals. Mean of N > 100 flies. *** $p < 0.001$.

In a previous work, pan-neural downregulation of dStim or dOrai has been shown to cause a significant reduction of SOCE and $[Ca^{2+}]_{ER}$ in primary neuronal cultures (Venkiteswaran and Hasan, 2009). In these flies, a reduced SOCE has been shown to affect neuronal functions, in particular their flight ability (Agrawal et al., 2010; Pathak et al., 2015). In order to assess whether the defect in SOCE observed upon spastin^{K467R} expression was likewise associated with an impairment in flight, the “cylinder drop” assay was performed. Flies were dropped into a one-meter long cylinder leading to an ethanol filled chamber and the number of surviving and dead flies was counted. Only flies with normal flight machinery are able to fly and potentially attach to the cylinder wall, while flies with impaired flight would drop into the ethanol chamber. An evident defect in the flight ability of spastin^{K467R} expressing flies was observed (42% reduction of spastin^{K467R} compared to control, $p < 0.001$; n = 100 control flies; n = 100 spastin^{K467R} flies;). Importantly, this defect was partially rescued when flies were raised in vinblastine-containing food (Figure 13E).

Altogether, these results indicate that a proper MT organization is required to maintain proper ER morphology and Ca^{2+} entry upon stores depletion. When the latter is impaired, flight ability is compromised. Strikingly, all the phenotypes caused by spastin^{K467R} expression were recovered upon treatment with vinblastine.

Neuronal dowregulation of Rtnl1 affects SOCE

The results presented so far describe the impairment of ER morphology and SOCE due to expression of spastin^{K467R}, and demonstrate they are all dependent on mutant spastin-induced MT hyperstabilization. The process of SOCE likely depends on a proper organization of both the tubular ER and MT cytoskeleton. In order to investigate whether ER tubules impairment *per se* could cause a

defective SOCE, we exploited a transgenic Drosophila line for the downregulation of Rtnl1 (UAS-Rtnl1-RNAi). It is indeed known that loss of Rtnl1, whose reported function is the structural maintenance of the tubular shape of the ER (Shibata et al., 2008; Zurek et al., 2011), causes an enrichment of ER sheets at the expenses of tubules (O'Sullivan et al., 2012). This alteration is reminiscent of the morphological change induced by spastin^{K467R} expression, without however dramatically affecting MT cytoskeleton. Indeed, it has been shown that loss of fly *Rtnl1* leads to a partial decrease of the MT marker Futsch; however the defect was very mild and localized only in the distal portions of long motor axons (O'Sullivan et al., 2012). Interestingly, it has been reported in a non-neuronal mammalian cell line that knock-out of Rtn4, one of the four human paralogs of Reticulon protein family, induces an enrichment of ER sheets at the expenses of tubules, which results in a decrease of SOCE (Jozsef et al., 2014).

Lifespan of flies downregulating Rtnl1 specifically in the nervous system (UAS-Rtnl1-RNAi/elav-Gal4) was evaluated as detailed before. A significant decrease in viability during ageing was observed, compared to controls (Figure 14A). Moreover, Rtnl1-RNAi flies displayed a faster decline in negative geotaxis during ageing, when compared to controls (Figure 14B). These results show that in neurons the downregulation of Rtnl1, similar to the expression of spastin^{K467R}, impairs fly viability and locomotor capacity.

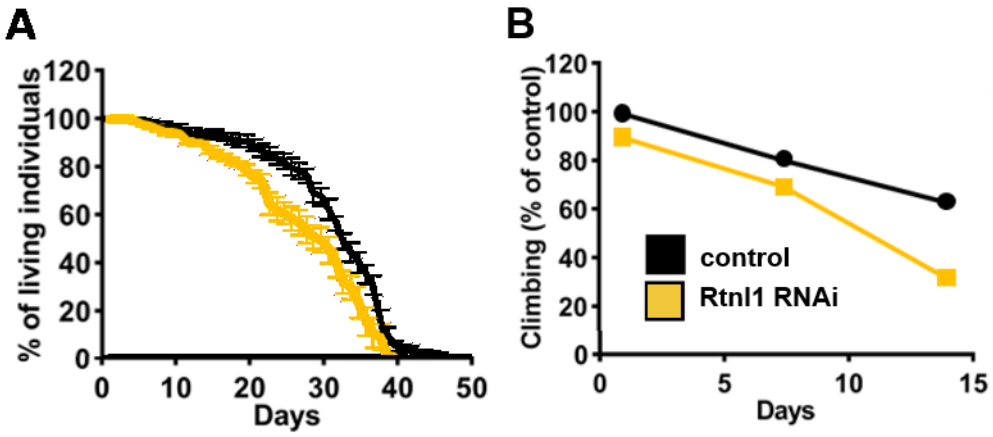

Figure 14. (A) Evaluation of fly survival: flies were separated in tubes (20 individuals/each) and counted every 2 days during ageing. Data represented as percentage of living flies over 40 days. **(B)** Evaluation of fly climbing ability: flies were tapped at the bottom of a graduated tube. Flies able to cross a 10 cm mark in 60 s were counted as climbing flies. Data shown as percentage of flies able to cross the line at day 1, 7 and 14.

The presence of morphological ER alterations in larval neurons downregulating Rtnl1 was confirmed by EM analysis of thin brain slices. EM images confirmed an increase in the length of ER profiles in Rtnl1-RNAi neurons, compared to control, consistent with an increase in ER sheets (Puhka et al., 2012) (Figure 15A-B). As expected, this shape remodeling is reminiscent of that observed in spastin^{K467R}-expressing neurons, although the downregulation of Rtnl1 does not cause a dramatic rearrangement of the cytoskeleton, at least in the cell body. To investigate whether a similar ER shape defect could result in comparable alterations of Ca^{2+} homeostasis, in particular SOCE, neurons were dissociated from Rtnl1-downregulated and control larval brains and loaded with fura-2. The experimental protocol to elicit SOCE, described before, was then applied to the cells. Ca^{2+} entry following stores depletion was significantly decreased in Rtnl1-downregulated neurons, compared to controls (Figure 15C-D). Accordingly, the cylinder drop test highlighted a defect in the flight ability of Rtnl1-RNAi flies (10% reduction compared to control, $p < 0.001$; n = 100 control flies; n = 100 Rtnl1 RNAi flies; Figure 15E).

This data corroborates the idea that a correct shape is necessary for proper ER function and, in particular, that ER sheets predominance impacts on a specific ER function which relies on the presence and physical movement of ER tubules towards the PM, namely SOCE.

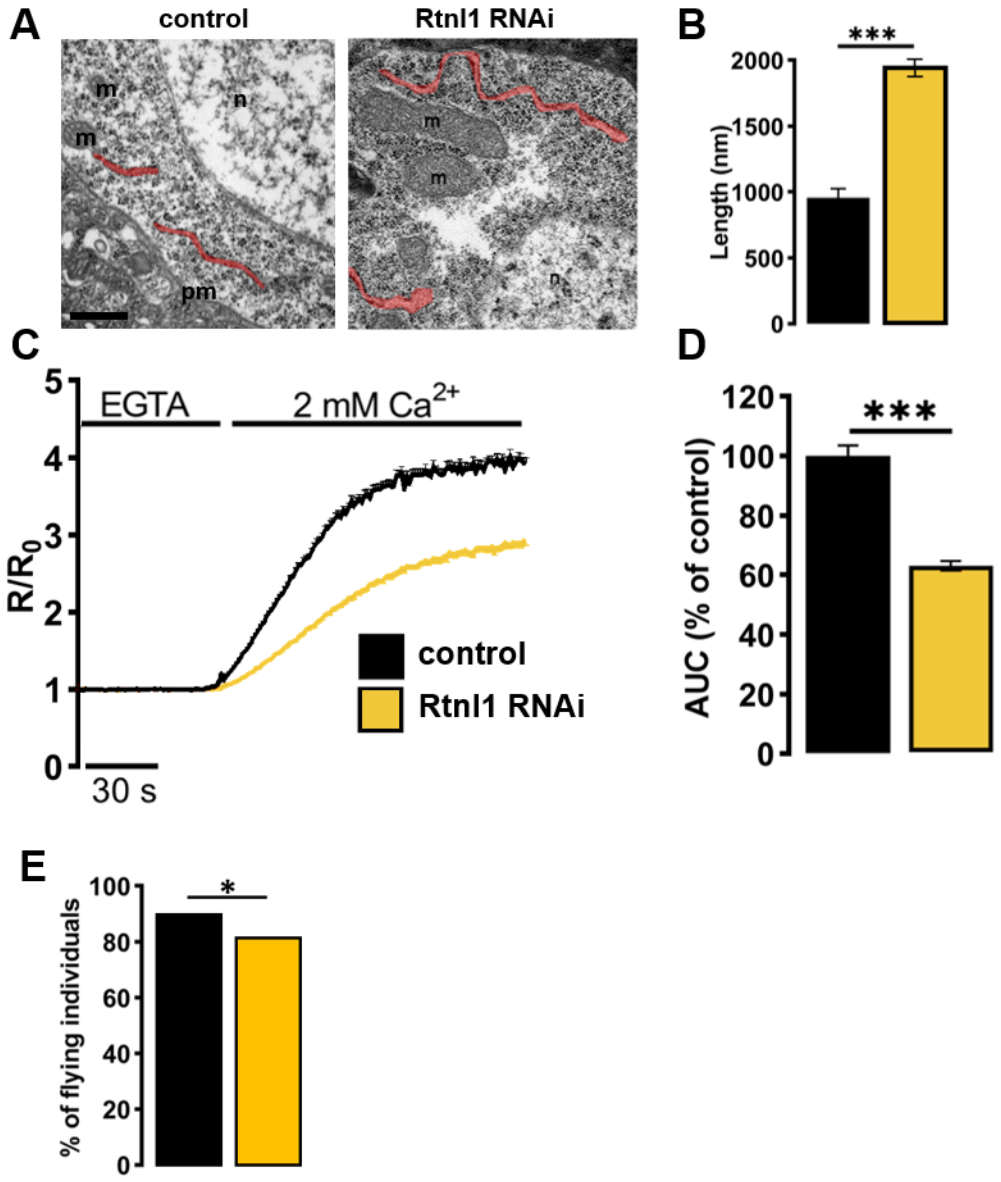

Figure 15. (A) Transmission electron microscopy (TEM) images of ventral ganglion neuronal cell bodies of Rtnl1-RNAi larvae and relative control; ER profiles are highlighted in red. pm, plasma membrane; n, nucleus; m, mitochondria. Scale bar, 500 nm. **(B)** Quantification of ER profiles' mean length of the indicated genotypes. Mean ± SEM, N ≥ 50. *** $p < 0.001$. **(C)** Cytosolic Ca^{2+} dynamics induced by SOCE activation in neurons dissociated from larval brains of the indicated genotypes, as detected by fura-2. Cells were pre-treated with thapsigargin in a Ca^{2+}-free medium for 8 min, to empty

intracellular Ca^{2+} stores, and then 2 mM $CaCl_2$ was added. Average traces are represented as R/R_0 of N > 100 cells. **(D)** Histograms report the average area under curve (AUC) of the traces recorded. **(E)** Flight ability, assayed by the cylinder drop test, of Rtnl1-RNAi animals and relative controls. Data are presented as the percentage of flying individuals. Mean of N > 100 flies. *** $p < 0.001$.

Discussion

It is widely assumed that ER structural heterogeneity contributes to its functional compartmentalization. Even though a clear-cut attribution of function to either sheets or tubules has yet to be defined, tubules appear to perform some specific functions. The involvement of TAC-mediated movement on MT tips suggests that the regulated process of SOCE depends specifically on ER tubules. Nevertheless, the influence of neuronal ER architecture on the process of SOCE and the molecular mechanisms of cytoskeleton regulation over the relocation of STIM to ER-PM junctions are not fully understood. It appears clear that the coordinated interplay between different molecules is necessary to mediate the transient formation of ER-PM junctions (Grigoriev et al., 2008; Maléth et al., 2014; Sharma et al., 2013; Woo et al., 2016), but whether the integrity of cytoskeleton is needed for proper SOCE activation is not clear. Opposing data are present in literature, suggesting both inhibition (Oka et al., 2005; Smyth et al., 2007) or potentiation (Galán et al., 2011) of SOCE in the presence of MT-depolymerizing agents. Even less is known about the requirement for SOCE of a proper ER network organization. A correlation between ER structure and the process of SOCE can be inferred from a few studies in non-neuronal mammalian cells showing that downregulation of human Reticulon-4 (Jozsef et al., 2014) or either overexpression or depletion of human Atlastin-1 (Li et al., 2017) cause an impairment in SOCE.

To explore the effect of ER morphology on SOCE in neurons, I set up an *in vivo* approach in *Drosophila melanogaster*. By manipulating specific proteins involved in the maintenance of proper ER or MT structure, I obtained experimental animal models with alterations in ER shape or MT dynamics, likely resulting in changed ER network distribution.

To affect MT structure, I expressed in Drosophila a variant of the MT-severing protein spastin carrying an amino acid substitution known to function as a

dominant negative, thus inducing MT hyper-stabilization. Interestingly, spastin^{K467R}-induced MT stabilization causes a change in ER morphology, shifting ER sheets/tubules balance toward the formation of sheets. The results I obtained in fly neurons clearly demonstrate the process of Ca^{2+} entry upon ER Ca^{2+} depletion negatively affected by spastin^{K467R} expression. This impairment results in a reduced ER Ca^{2+} content without, however, affecting cytosolic basal Ca^{2+} levels.

These phenotypes recapitulate those observed upon dStim or dOrai downregulation in flies. Pan-neural downregulation of dStim or dOrai leads to a significant reduction of SOCE and $[Ca^{2+}]_{ER}$ in primary larval neurons (Venkiteswaran and Hasan, 2009). Reduced SOCE has been shown to affect fly neuronal functions, in particular a significant loss of flight has been observed, accompanied by the loss of rhythmic flight patterns (Venkiteswaran and Hasan, 2009), indicating that, in neurons, the correct refilling of intracellular Ca^{2+} stores is required for Drosophila flight. A similar defect in flight ability, tested in the cylinder drop assay, was observed also in flies expressing spastin^{K467R}. This phenotype is specific, since dSERCA mutant flies, in which stored Ca^{2+} is decreased but SOCE is increased, do not display flight defects (Banerjee et al., 2006; Venkiteswaran and Hasan, 2009).

Beneficial effects from treatments with vinblastine have been reported in flies expressing spastin^{K467R} (Orso et al., 2005). By recovering MT organization, vinblastine rescues NMJs morphology and function, together with fly viability and climbing defects (Orso et al., 2005). Here, I showed that vinblastine treatment can rescue also ER morphology, Ca^{2+} handling defects and flight ability, indicating that MT impairment is the earliest responsible for the observed phenotypes. Notably, acute vinblastine treatment (50 minutes application on dissociated neurons) is sufficient to rescue SOCE and ER Ca^{2+} content. Within this time-window, transcriptional activation is unlikely to occur, suggesting that the levels of Ca^{2+} handling proteins are unaltered and the defects observed are directly ascribable to MT dynamics impairment.

The data obtained allows us to speculate that MT disorganization and SOCE impairment are causally linked to the observed ER morphology alterations induced by spastin^{K467R} expression in flies: MT hyper-stabilization shifts the ER sheet/tubule balance in favour of ER sheets; this, in turn, affects SOCE, a specific ER function that relies on the physical movement of ER tubules towards the PM.

MT dynamics itself is critical to generate pushing and pulling forces during their polymerization and depolymerization, respectively (Inoué and Salmon, 1995) providing the force required for membrane movement that can result in membrane translocation from one point to another within the cell. For this reason, I cannot exclude that MT impairment *per se* is responsible for the observed reduction of SOCE. The rescue of MT network upon vinblastine treatment recovers also ER morphology in spastin^{K467R} expressing flies, hindering the separation of the contribution of ER or MT network in maintaining a proper SOCE. The non-complete recovery of SOCE upon vinblastine treatment, however, indicates that the structural integrity of both ER and MT is not sufficient. Further studies are required to investigate the SOC machinery proteins level and distribution in the recovered ER. Nevertheless, our results indicate that the integrity of both structures is a necessary requirement for a functional SOCE.

Indeed, the necessity of an intact ER network for a functional SOCE to occur emerges from the results I obtained upon downregulation of Rtnl1. In this model, the protein responsible for ER tubules formation and maintenance is absent and the ER experiences an increase in sheet-like structures. The modification of ER shape is thus similar to that obtained upon expression of spastin^{K467R}, however in this case MT cytoskeleton is not dramatically affected. Interestingly, I also observed a similar impairment in SOCE upon downregulation of Rtnl1, suggesting that ER shape alteration, and in particular the enrichment in cisternal components, is the primary cause of Ca^{2+} entry reduction.

Ca^{2+} signals regulate fundamental aspects of neuronal function and physiology and contribute in determining the morphology of neural circuits (Berridge, 1998; Borodinsky and Spitzer, 2007). Traditionally, most of these signals have been attributed to the entry of extracellular Ca^{2+} through voltage-operated channels or

ionotropic receptors. However, components of the "Ca^{2+} toolkit" coupled to Ca^{2+} release from intracellular stores are present in neurons. Our results corroborate growing evidence suggesting that also neurons rely on SOCE and its dysregulation may participate in the pathogenesis of diverse neurodegenerative diseases, such as Alzheimer's, Parkinson's, Charcot-Marie-Tooth disease (Secondo et al., 2018).

Indeed, a common thread linking the two genes object of this study is that their mutation causes the neurodegenerative disorder HSP. The initially proposed pathogenetic mechanism for the disease relied on impaired axonal transport, which would be detrimental for the body's longest axons; however, this explanation appears not adequate since evidence showed that degeneration can also affect very short axons. Interestingly, despite the genetic heterogeneity of HSPs, alterations in morphology and/or distribution of the ER appear to be a critical causative factor, as over 60% of HSP patients carries mutations in genes encoding proteins that act on ER morphology, either directly or affecting its cellular distribution (Fink, 2013; Lo Giudice et al., 2014).

In neurons, the potential link between ER structure and function has never been explored in detail. Neurons are particularly dependent on an elaborate ER network for proper functionality. Their unique architecture requires an elongated peripheral ER network that extends in both axons and dendrites. Moreover, the link between ER morphology/function defects and the onset of HSPs have not been elucidated. The results here described support the idea that the impact of diverse HSP proteins on ER shape could be causative of a common alteration of ER function. Altogether, these observations place the ER at the nexus of HSP pathology, suggesting that ER functionality is likely critical for neuronal degeneration associated to HSP. The identification of common alterations in Ca^{2+} homeostasis caused by ER morphology impairment, induced via distinct mechanisms, will set the basis for establishing a role for Ca^{2+} dyshomeostasis in the pathogenesis of HSP.

Materials and Methods

Drosophila stocks and crosses

The UAS-Dspastin-K467R and UAS-BiP-sf-GFP-ER fly lines used in this study were described previously (Orso et al., 2005; Summerville et al., 2016). TheUAS-Rtnl1RNAi fly line was obtained from the Bloomington Drosophila Stock Center (NIH P40OD018537). The Gal4 strains used for the expression were: Elav-Gal4 (pan neuronal expression); D42-Gal4 (motor neurons restricted), both obtained from Bloomington Drosophila Stock Center. To increase protein expression, all experimental crosses were performed at 28°C. Control genotypes included promoter-Gal4/+ individuals. Fly food was prepared using NUTRI-fly-IF mixture (Genesee Scientific), according to the manufacturer instructions. For chronic vinblastine treatment, 50 nM vinblastine was mixed with NUTRI-fly-IF.

Transmission electron microscopy

Drosophila brains and were fixed in 4% paraformaldehyde and 2% glutaraldehyde and embedded as described earlier. EM images were acquired from thin sections under a Philips Tecnai-12 electron microscope using an ULTRA VIEW CCD digital camera (Soft Imaging Systems GmbH). EM images of individual neurons for the measurement of the length of ER profiles were collected from three brains for each genotype. In total, 26 spastin^{K467R}, 40 Rtnl1 RNAi and 20 control neurons were analyzed. In the rescue experiment a total of 50 neurons expressing spastin^{K467R} were analyzed. Quantitative analyses were performed with GraphPad Prism 8.

Confocal images of larval brains

Brains and ventral ganglia from third instar larvae expressing BiP-sf-GFP-ER alone or together with spastin^{K467R} were dissected in M1 medium (see below) containing 1mM Ca^{2+}, immobilized on a mounting slide and covered with a drop of the dissecting solution and a coverslip. Imaging of living motor neuron cell bodies was performed for on a Leica TCS SP5 II confocal microscope equipped with an HCX PL APO lambda blue 63x/1.40-0.60 Oil objective, using a 488 nm laser. Once acquired, background subtraction was carried out using ImageJ plug-ins.

Preparation of larval neurons

Larval neurons were dissociated as previously reported (Chakraborty and Hasan, 2018). Briefly, third instar larvae were collected in a Petri dish, rinsed once with double-distilled water, twice with 70% ethanol, then with M3 complete medium (Shields and Sang M3 Insect Medium, supplemented with 10% heat-inactivated FBS, 50 U/mL penicillin, 50 µg/mL streptomycin). Brains were dissected with sterilized forceps under a light microscope. Brains were centrifuged at washed twice with M3 complete medium, then transferred to an enzymatic solution (0.75 µg/µL collagenase A and 0.4 µg/µL dispase II in M3 complete medium) and incubated for 20 min at room temperature in agitation. During incubation, brains were mechanically dissociated by gentle pipetting. Cell lysates were centrifuged at 600 × g for 5 min in a table top centrifuge and washed twice with dissecting solution to remove any residual enzymes. The cell pellet was resuspended with 100 µL of M3 complete medium for each brain; 100 µL were plated for each coverslip, approximately corresponding to one brain. Coverslips were previously autoclaved and coated with a drop of 0.1 mg/ml of poly-L-lysine for 30 min at 37°C.

Climbing assay

Climbing assay was performed as previously described (Agrawal and Hasan, 2015) using a glass cylinder with a diameter of 2.5 cm. Flies of the indicated

genotype were dropped in the cylinder in batches of 20 at one, seven and fourteen day after pupal eclosion. A gentle tap was given three times so that all the flies reach the bottom of the cylinder. Then the number of flies that crossed a 10 cm mark in 60 s were counted manually. Each batch of flies was tested three times. Means were calculated counting the total number of climbing flies for each repetition and an independent proportion analysis was used to determine differences between populations.

Flight assay

The flight assay was adapted from a previously published protocol (Banerjee, 2004) using a 1 m long, Plexiglas cylinder (diameter 5 cm) connected with an ethanol filled chamber at the bottom. Groups of 20 flies of a selected genotype were dropped into the cylinder through the top entry. A fly was determined to be capable of flight if it manages to reach the cylinder wall. Flies that could not perform this task fell directly into the ethanol filled chamber. Flight assays were performed on day 7 after pupal eclosion. Data represent the percentage of flies capable of flight, at least 100 flies per condition were tested. Independent proportion analysis was used to determine the differences between groups.

Cytosolic Ca^{2+} imaging

Neuronal cells were incubated with fura-2/AM (1 μM), pluronic F-127 (0.02%), and sulfinpyrazone (200 μM) for 20 min at room temperature (RT) in a M1 buffer (in mM: 30 HEPES, 150 NaCl, 5 KCl, 1 $MgCl_2$, 1 $CaCl_2$, 35 sucrose, and 5 glucose at pH 7.2) and then in a fresh solution without the Ca^{2+} indicator for 20 minutes at RT. Fura-2–loaded cells were visualized with a 20x ultraviolet-permeable objective (CFI Sfluor 20x N.A. 0.75, Nikon) on an inverted microscope (Nikon Ti-E). Fluorescence illumination was achieved by 50-75W Lamp (USHIO UXLS50A) and alternating excitation wavelengths (340/380 nm) were obtained by a monochromator (Optoscan CAIRN-Research) controlled by NIS-ELEMENTS AR (Nikon) software. A neutral density filter, ND4 (Nikon, USA), and a FF-409-DiO3

Dichroic mirror (Semrock) were used in the excitation pathway. The emitted fluorescence was collected using and a 510/84nm (Semrock) filter. Images were acquired every 1 s, with 100ms exposure time at each wavelength, by a Zyla-CMOS 4.2-P (Andor, Oxford Instruments) controlled by the same software. During the experiment, cells plated on coverslips were mounted into an open-topped chamber and maintained in an extracellular-like medium containing the following:

1) M1 (Na^+-based) medium: 30 mM HEPES, 150 mM NaCl, 5 mM KCl, 1 mM MgCl2, 35 mM sucrose, pH 7.2 with NaOH at RT;

2) K^+-based medium: 30 mM HEPES, 145 mM K-D-gluconate, 10 mM NaCl, 1 mM $MgCl_2$, 35 mM sucrose, 5 mM glucose pH 7.2 with KOH at RT.

For store Ca^{2+} content evaluation, cells were firstly perfused with M1 containing 1 mM $CaCl_2$; after addition of 500 µM EGTA, cells were stimulated by addition of ionomycin (10 µM) or cyclopiazonic acid (CPA, 50 µM). In the second case, for residual Ca^{2+} evaluation, cells were further stimulated with addition of ionomycin (10 µM). For SOCE activation experiments, cells were pre-treated with the irreversible SERCA inhibitor thapsigargin (100 nM) for 10 min in a Ca^{2+}-free, EGTA (500 µM)-containing M1; cells were then perfused with the same medium without the SERCA inhibitor and challenged with $CaCl_2$ (2 or 5 mM). Where indicated, M1 (Na^+-based) medium was substituted with K^+-based medium.

For acute vinblastine treatment, the drug (1µM) was added in each solution and step of the experimental protocol, from fura-2/AM cell loading to cell stimulations. Neurons dissociated from larvae exposed to chronic vinblastine treatment, were similarly treated.

Ca^{2+} imaging experiments analysis

Off-line analysis of Ca^{2+} imaging experiments was performed using the NIS-Elements software. F_{340} and F_{380} images were subtracted of background signals and proper regions of interest (ROIs) were selected on each imaged cell. The

ratio of the emitted fluorescence intensities ($R = F_{340}/F_{380}$) was calculated for each ROI, normalized to the value measured before stimulus addition, or at the Ca^{2+}-free status, and averaged offline. Data were analyzed using Microsoft Excel and Graphpad Prism 8 to calculate areas under the curves (AUC).

Statistical analyses

Fura-2 traces represent average values of 100 to 1000 cells collected in 3–10 independent experiments. Average values are expressed as mean ± standard error of the mean (n = number of cells, unless otherwise specified). Statistical analyses were performed using unpaired Student's t-test. Analyses of differences between fly populations were made using chi-square independent proportion analysis. Both tests were applied with a confidence interval of 95% (*$p < 0.05$, **$p < 0.01$, ***$p<0.001$).

Materials

Shields and Sang M3 Insect Medium, Dispase II, vinblastine, thapsigargin, EGTA and $CaCl_2$ were purchased from Sigma-Aldrich. CPA, and ionomycin were purchased from Abcam, Collagenase A was purchased from Roche. Fura-2/AM was purchased from Thermo Fisher. All other materials were analytical or of the highest available grade.

Bibliography

Agostini, M., and Fasolato, C. (2016). When, where and how? Focus on neuronal calcium dysfunctions in Alzheimer's Disease. *Cell Calcium*. doi:10.1016/j.ceca.2016.06.008.

Agrawal, N., Venkiteswaran, G., Sadaf, S., Padmanabhan, N., Banerjee, S., and Hasan, G. (2010). Inositol 1,4,5-trisphosphate receptor and dSTIM function in Drosophila insulin-producing neurons regulates systemic intracellular calcium homeostasis and flight. *J. Neurosci.* doi:10.1523/JNEUROSCI.3668-09.2010.

Agrawal, T., and Hasan, G. (2015). Maturation of a central brain flight circuit in Drosophila requires Fz2/Ca2+ signaling. *Elife* 4. doi:10.7554/elife.07046.

Allan, V. J., and Vale, R. D. (1991). Cell cycle control of microtubule-based membrane transport and tubule formation in vitro. *J. Cell Biol.* doi:10.1083/jcb.113.2.347.

Alushin, G. M., Lander, G. C., Kellogg, E. H., Zhang, R., Baker, D., and Nogales, E. (2014). High-Resolution microtubule structures reveal the structural transitions in αβ-tubulin upon GTP hydrolysis. *Cell*. doi:10.1016/j.cell.2014.03.053.

Anderson, D. J., and Hetzer, M. W. (2008). Shaping the endoplasmic reticulum into the nuclear envelope. *J. Cell Sci.* doi:10.1242/jcs.005777.

Anwar, K., Klemm, R. W., Condon, A., Severin, K. N., Zhang, M., Ghirlando, R., et al. (2012). The dynamin-like GTPase Sey1p mediates homotypic ER fusion in S. cerevisiae. *J. Cell Biol.* doi:10.1083/jcb.201111115.

Audhya, A., Desai, A., and Oegema, K. (2007). A role for Rab5 in structuring the endoplasmic reticulum. *J. Cell Biol.* doi:10.1083/jcb.200701139.

Baas, P. W., Nadar, C. V., and Myers, K. A. (2006). Axonal transport of microtubules: The long and short of it. *Traffic*. doi:10.1111/j.1600-0854.2006.00392.x.

Bai, J., Binari, R., Ni, J. Q., Vijayakanthan, M., Li, H. S., and Perrimon, N. (2008). RNA interference screening in Drosophila primary cells for genes involved in muscle assembly and maintenance. *Development*. doi:10.1242/dev.012849.

Banerjee, S. (2004). Loss of Flight and Associated Neuronal Rhythmicity in Inositol 1,4,5-

Trisphosphate Receptor Mutants of Drosophila. *J. Neurosci.* doi:10.1523/jneurosci.0656-04.2004.

Banerjee, S., Joshi, R., Venkiteswaran, G., Agrawal, N., Srikanth, S., Alam, F., et al. (2006). Compensation of Inositol 1,4,5-Trisphosphate Receptor Function by Altering Sarco-Endoplasmic Reticulum Calcium ATPase Activity in the Drosophila Flight Circuit. *J. Neurosci.* doi:10.1523/jneurosci.1231-06.2006.

Baumann, O., and Walz, B. (2001). Endoplasmic reticulum of animal cells and its organization into structural and functional domains. *Int. Rev. Cytol.* doi:10.1016/S0074-7696(01)05004-5.

Beetz, C., Nygren, A. O. H., Schickel, J., Auer-Grumbach, M., Bürk, K., Heide, G., et al. (2006). High frequency of partial SPAST deletions in autosomal dominant hereditary spastic paraplegia. *Neurology*. doi:10.1212/01.wnl.0000244413.49258.f5.

Benyamini, P., Webster, P., and Meyer, D. I. (2009). Knockdown of p180 eliminates the terminal differentiation of a secretory cell line. *Mol. Biol. Cell*. doi:10.1091/mbc.E08-07-0682.

Berridge, M. J. (1998). Neuronal calcium signaling. *Neuron*. doi:10.1016/S0896-6273(00)80510-3.

Berry, J. A., Cervantes-Sandoval, I., Chakraborty, M., and Davis, R. L. (2015). Sleep Facilitates Memory by Blocking Dopamine Neuron-Mediated Forgetting. *Cell*. doi:10.1016/j.cell.2015.05.027.

Betancourt-Solis, M. A., Desai, T., and McNew, J. A. (2018). The atlastin membrane anchor forms an intramembrane hairpin that does not span the phospholipid bilayer. *J. Biol. Chem.* doi:10.1074/jbc.RA118.003812.

Bezprozvanny, I., and Hayden, M. R. (2004). Deranged neuronal calcium signaling and Huntington disease. *Biochem. Biophys. Res. Commun.* doi:10.1016/j.bbrc.2004.08.035.

Blackstone, C. (2012). Cellular Pathways of Hereditary Spastic Paraplegia. *Annu. Rev. Neurosci.* doi:10.1146/annurev-neuro-062111-150400.

Blackstone, C., O'Kane, C. J., and Reid, E. (2011). Hereditary spastic paraplegias:

Membrane traffic and the motor pathway. *Nat. Rev. Neurosci.* doi:10.1038/nrn2946.

Borodinsky, L. N., and Spitzer, N. C. (2007). Activity-dependent neurotransmitter-receptor matching at the neuromuscular junction. *Proc. Natl. Acad. Sci.* doi:10.1073/pnas.0607450104.

Boucher, D., Larcher, J. C., Gros, F., and Denoulet, P. (1994). Polyglutamylation of Tubulin as a Progressive Regulator of in Vitro Interactions between the Microtubule-Associated Protein Tau and Tubulin. *Biochemistry*. doi:10.1021/bi00207a014.

Boulianne, G. L., Livne-Bar, I., Humphreys, J. M., Liang, Y., Lin, C., Rogaev, E., et al. (1997). Cloning and characterization of the Drosophila presenilin homologue. *Neuroreport*. doi:10.1097/00001756-199703030-00041.

Brand, A. H., and Perrimon, N. (1993). Targeted gene expression as a means of altering cell fates and generating dominant phenotypes. *Development*.

Bridges, C. B., and Morgan, T. H. (2012). *Sex-linked inheritance in Drosophila,*. doi:10.5962/bhl.title.54326.

Campàs, O., Leduc, C., Bassereau, P., Casademunt, J., Joanny, J. F., and Prost, J. (2008). Coordination of kinesin motors pulling on fluid membranes. *Biophys. J.* doi:10.1529/biophysj.107.118554.

Carrasco, S., and Meyer, T. (2011). STIM Proteins and the Endoplasmic Reticulum-Plasma Membrane Junctions. *Annu. Rev. Biochem.* 80, 973–1000. doi:10.1146/annurev-biochem-061609-165311.

Cepeda, C., Ariano, M. A., Calvert, C. R., Flores-Hernández, J., Chandler B, S. H., Leavitt, B. R., et al. (2001). NMDA receptor function in mouse models of Huntington disease. *J. Neurosci. Res.* doi:10.1002/jnr.1244.

Chakraborty, S., and Hasan, G. (2018). “Store-Operated Ca2+ Entry in Drosophila Primary Neuronal Cultures,” in *Methods in Molecular Biology* doi:10.1007/978-1-4939-8704-7_11.

Chen, S., Desai, T., McNew, J. A., Gerard, P., Novick, P. J., and Ferro-Novick, S. (2015). Lunapark stabilizes nascent three-way junctions in the endoplasmic reticulum. *Proc. Natl. Acad. Sci.* 112, 418–423. doi:10.1073/pnas.1423026112.

Chen, S., Novick, P., and Ferro-Novick, S. (2012). ER network formation requires a balance of the dynamin-like GTPase Sey1p and the Lunapark family member Lnp1p. *Nat. Cell Biol.* doi:10.1038/ncb2523.

Chen, Y. T., Chen, Y. F., Chiu, W. T., Liu, K. Y., Liu, Y. L., Chang, J. Y., et al. (2013). Microtubule-associated histone deacetylase 6 supports the calcium store sensor STIM1 in mediating malignant cell behaviors. *Cancer Res.* doi:10.1158/0008-5472.CAN-12-4127.

Chiurchiù, V., Maccarrone, M., and Orlacchio, A. (2014). The role of reticulons in neurodegenerative diseases. *NeuroMolecular Med.* doi:10.1007/s12017-013-8271-9.

Choi, S., Quan, X., Bang, S., Yoo, H., Kim, J., Park, J., et al. (2017). Mitochondrial calcium uniporter in Drosophila transfers calcium between the endoplasmic reticulum and mitochondria in oxidative stress-induced cell death. *J. Biol. Chem.* doi:10.1074/jbc.M116.765578.

Chorna, T., and Hasan, G. (2012). The genetics of calcium signaling in Drosophila melanogaster. *Biochim. Biophys. Acta - Gen. Subj.* doi:10.1016/j.bbagen.2011.11.002.

Clark, I. E., Dodson, M. W., Jiang, C., Cao, J. H., Huh, J. R., Seol, J. H., et al. (2006). Drosophila pink1 is required for mitochondrial function and interacts genetically with parkin. *Nature*. doi:10.1038/nature04779.

Claudiani, P., Riano, E., Errico, A., Andolfi, G., and Rugarli, E. I. (2005). Spastin subcellular localization is regulated through usage of different translation start sites and active export from the nucleus. *Exp. Cell Res.* doi:10.1016/j.yexcr.2005.06.009.

Coombes, C. E., Yamamoto, A., Kenzie, M. R., Odde, D. J., and Gardner, M. K. (2013). Evolving tip structures can explain age-dependent microtubule catastrophe. *Curr. Biol.* doi:10.1016/j.cub.2013.05.059.

Dabora, S. L., and Sheetz, M. F. (1988). The microtubule-dependent formation of a tubulovesicular network with characteristics of the ER from cultured cell extracts. *Cell*. doi:10.1016/0092-8674(88)90176-6.

Dayel, M. J., Horn, E. F. Y., and Verkman, A. S. (1999). Diffusion of green fluorescent

protein in the aqueous-phase lumen of endoplasmic reticulum. *Biophys. J.* doi:10.1016/S0006-3495(99)77438-2.

De Craene, J. O., Coleman, J., De Martin, P. E., Pypaert, M., Anderson, S., Yates, J. R., et al. (2006). Rtn1p Is involved in structuring the cortical endoplasmic reticulum. *Mol. Biol. Cell*. doi:10.1091/mbc.E06-01-0080.

Desai, A., and Mitchison, T. J. (1997). Microtubule Polymerization Dynamics. *Annu. Rev. Cell Dev. Biol.* 13, 83–117. doi:10.1146/annurev.cellbio.13.1.83.

DiAntonio, A. (2006). Glutamate Receptors At The Drosophila Neuromuscular Junction. *Int. Rev. Neurobiol.* doi:10.1016/S0074-7742(06)75008-5.

Dimitrov, A., Quesnoit, M., Moutel, S., Cantaloube, I., Poüs, C., and Perez, F. (2008). Detection of GTP-tubulin conformation in vivo reveals a role for GTP remnants in microtubule rescues. *Science (80-.).* doi:10.1126/science.1165401.

Drago, I., and Davis, R. L. (2016). Inhibiting the Mitochondrial Calcium Uniporter during Development Impairs Memory in Adult Drosophila. *Cell Rep.* doi:10.1016/j.celrep.2016.08.017.

Dreier, L., and Rapoport, T. A. (2000). In vitro formation of the endoplasmic reticulum occurs independently of microtubules by a controlled fusion reaction. *J. Cell Biol.* doi:10.1083/jcb.148.5.883.

Eckert, T., Link, S., Tuong-Van Le, D., Sobczak, J. P., Gieseke, A., Richter, K., et al. (2012). Subunit interactions and cooperativity in the microtubule-severing AAA ATPase spastin. *J. Biol. Chem.* doi:10.1074/jbc.M111.291898.

English, A. R., Zurek, N., and Voeltz, G. K. (2009). Peripheral ER structure and function. *Curr. Opin. Cell Biol.* doi:10.1016/j.ceb.2009.04.004.

Erck, C., Peris, L., Andrieux, A., Meissirel, C., Gruber, A. D., Vernet, M., et al. (2005). A vital role of tubulin-tyrosine-ligase for neuronal organization. *Proc. Natl. Acad. Sci. U. S. A.* doi:10.1073/pnas.0409626102.

Errico, A., Ballabio, A., and Rugarli, E. I. (2002). Spastin, the protein mutated in autosomal dominant hereditary spastic paraplegia, is involved in microtubule dynamics. *Hum. Mol. Genet.* 11, 153–63.

Evans, K. J., Gomes, E. R., Reisenweber, S. M., Gundersen, G. G., and Lauring, B. P. (2005). Linking axonal degeneration to microtubule remodeling by Spastin-mediated microtubule severing. *J. Cell Biol.* doi:10.1083/jcb.200409058.

Evans, K., Keller, C., Pavur, K., Glasgow, K., Conn, B., and Lauring, B. (2006). Interaction of two hereditary spastic paraplegia gene products, spastin and atlastin, suggests a common pathway for axonal maintenance. *Proc. Natl. Acad. Sci. U. S. A.* doi:10.1073/pnas.0510863103.

Ewen-Campen, B., Yang-Zhou, D., Fernandes, V. R., González, D. P., Liu, L. P., Tao, R., et al. (2017). Optimized strategy for in vivo Cas9-activation in Drosophila. *Proc. Natl. Acad. Sci. U. S. A.* doi:10.1073/pnas.1707635114.

Farías, G. G., Fréal, A., Tortosa, E., Stucchi, R., Pan, X., Portegies, S., et al. (2019). Feedback-Driven Mechanisms between Microtubules and the Endoplasmic Reticulum Instruct Neuronal Polarity. *Neuron*. doi:10.1016/j.neuron.2019.01.030.

Fasolato, C., Zottini, M., Clementi, E., Zacchetti, D., Meldolesi, J., and Pozzan, T. (1991). Intracellular Ca2+ pools in PC12 cells: Three intracellular pools are distinguished by their turnover and mechanisms of Ca2+ accumulation, storage, and release. *J. Biol. Chem.*

Feany, M. B., and Bender, W. W. (2000). A Drosophila model of Parkinson's disease. *Nature*. doi:10.1038/35006074.

Feske, S., Gwack, Y., Prakriya, M., Srikanth, S., Puppel, S. H., Tanasa, B., et al. (2006). A mutation in Orai1 causes immune deficiency by abrogating CRAC channel function. *Nature*. doi:10.1038/nature04702.

Fink, J. K. (2013). Hereditary spastic paraplegia: Clinico-pathologic features and emerging molecular mechanisms. *Acta Neuropathol.* doi:10.1007/s00401-013-1115-8.

Friedman, J. R., Webster, B. M., Mastronarde, D. N., Verhey, K. J., and Voeltz, G. K. (2010). ER sliding dynamics and ER-mitochondrial contacts occur on acetylated microtubules. *J. Cell Biol.* doi:10.1083/jcb.200911024.

Fukushima, N., Furuta, D., Hidaka, Y., Moriyama, R., and Tsujiuchi, T. (2009). Post-translational modifications of tubulin in the nervous system. *J. Neurochem.*

doi:10.1111/j.1471-4159.2009.06013.x.

Galán, C., Dionisio, N., Smani, T., Salido, G. M., and Rosado, J. A. (2011). The cytoskeleton plays a modulatory role in the association between STIM1 and the Ca2+ channel subunits Orai1 and TRPC1. *Biochem. Pharmacol.* doi:10.1016/j.bcp.2011.05.017.

Gardner, M. K., Zanic, M., Gell, C., Bormuth, V., and Howard, J. (2011). Depolymerizing kinesins Kip3 and MCAK shape cellular microtubule architecture by differential control of catastrophe. *Cell*. doi:10.1016/j.cell.2011.10.037.

Giorgi, C., Danese, A., Missiroli, S., Patergnani, S., and Pinton, P. (2018). Calcium Dynamics as a Machine for Decoding Signals. *Trends Cell Biol.* doi:10.1016/j.tcb.2018.01.002.

Goate, A., Chartier-Harlin, M. C., Mullan, M., Brown, J., Crawford, F., Fidani, L., et al. (1991). Segregation of a missense mutation in the amyloid precursor protein gene with familial Alzheimer's disease. *Nature*. doi:10.1038/349704a0.

Goyal, U., and Blackstone, C. (2013). Untangling the web: Mechanisms underlying ER network formation. *Biochim. Biophys. Acta - Mol. Cell Res.* doi:10.1016/j.bbamcr.2013.04.009.

Grigoriev, I., Gouveia, S. M., van der Vaart, B., Demmers, J., Smyth, J. T., Honnappa, S., et al. (2008). STIM1 Is a MT-Plus-End-Tracking Protein Involved in Remodeling of the ER. *Curr. Biol.* doi:10.1016/j.cub.2007.12.050.

Grumati, P., Morozzi, G., Hölper, S., Mari, M., Harwardt, M. L. I. E., Yan, R., et al. (2017). Full length RTN3 regulates turnover of tubular endoplasmic reticulum via selective autophagy. *Elife*. doi:10.7554/eLife.25555.

Grynkiewicz, G., Poenie, M., and Tsien, R. Y. (1985). A new generation of Ca2+ indicators with greatly improved fluorescence properties. *J. Biol. Chem.*

Guo, Y., Li, D., Zhang, S., Yang, Y., Liu, J. J., Wang, X., et al. (2018). Visualizing Intracellular Organelle and Cytoskeletal Interactions at Nanoscale Resolution on Millisecond Timescales. *Cell*. doi:10.1016/j.cell.2018.09.057.

Hammond, J. W., Cai, D., and Verhey, K. J. (2008). Tubulin modifications and their cellular functions. *Curr. Opin. Cell Biol.* doi:10.1016/j.ceb.2007.11.010.

Hanus, C., and Ehlers, M. D. (2016). Specialization of biosynthetic membrane trafficking for neuronal form and function. *Curr. Opin. Neurobiol.* doi:10.1016/j.conb.2016.03.004.

Hardie, R. C., and Minke, B. (1992). The trp gene is essential for a light-activated Ca2+ channel in Drosophila photoreceptors. *Neuron*. doi:10.1016/0896-6273(92)90086-S.

Harkcom, W. T., Ghosh, A. K., Sung, M. S., Matov, A., Brown, K. D., Giannakakou, P., et al. (2014). NAD+ and SIRT3 control microtubule dynamics and reduce susceptibility to antimicrotubule agents. *Proc. Natl. Acad. Sci.* doi:10.1073/pnas.1404269111.

Hasan, G., and Rosbash, M. (1992). Drosophila homologs of two mammalian intracellular Ca2+-release channels: Identification and expression patterns of the inositol 1,4,5-triphosphate and the ryanodine receptor genes. *Development*.

Hazan, J., Fonknechten, N., Mavel, D., Paternotte, C., Samson, D., Artiguenave, F., et al. (1999). Spastin, a new AAA protein, is altered in the most frequent form of autosomal dominant spastic paraplegia. *Nat. Genet.* doi:10.1038/15472.

Hodgson, J. G., Agopyan, N., Gutekunst, C. A., Leavitt, B. R., Lepiane, F., Singaraja, R., et al. (1999). A YAC mouse model for Huntington's disease with full-length mutant huntingtin, cytoplasmic toxicity, and selective striatal neurodegeneration. *Neuron*. doi:10.1016/S0896-6273(00)80764-3.

Honnappa, S., Gouveia, S. M., Weisbrich, A., Damberger, F. F., Bhavesh, N. S., Jawhari, H., et al. (2009). An EB1-Binding Motif Acts as a Microtubule Tip Localization Signal. *Cell*. doi:10.1016/j.cell.2009.04.065.

Hu, J., Shibata, Y., Voss, C., Shemesh, T., Li, Z., Coughlin, M., et al. (2008). Membrane proteins of the endoplasmic reticulum induce high-curvature tubules. *Science (80-.).* doi:10.1126/science.1153634.

Hu, J., Shibata, Y., Zhu, P. P., Voss, C., Rismanchi, N., Prinz, W. A., et al. (2009). A Class of Dynamin-like GTPases Involved in the Generation of the Tubular ER Network. *Cell*. doi:10.1016/j.cell.2009.05.025.

Huang, Z., Ren, S., Jiang, Y., and Wang, T. (2016). PINK1 and Parkin cooperatively

protect neurons against constitutively active TRP channel-induced retinal degeneration in Drosophila. *Cell Death Dis.* doi:10.1038/cddis.2016.82.

Hyman, A. A., Chretien, D., Arnal, I., and Wade, R. H. (1995). Structural changes accompanying GTP hydrolysis in microtubules: Information from a slowly hydrolyzable analogue guanylyl-(??,??)-methylene- diphosphonate. *J. Cell Biol.*

Iijima, K., Liu, H. P., Chiang, A. S., Hearn, S. A., Konsolaki, M., and Zhong, Y. (2004). Dissecting the pathological effects of human Aβ40 and Aβ42 in Drosophila: A potential model for Alzheimer's disease. *Proc. Natl. Acad. Sci. U. S. A.* doi:10.1073/pnas.0400895101.

Ikegami, K., Heier, R. L., Taruishi, M., Takagi, H., Mukai, M., Shimma, S., et al. (2007). Loss of α-tubulin polyglutamylation in ROSA22 mice is associated with abnormal targeting of KIF1A and modulated synaptic function. *Proc. Natl. Acad. Sci. U. S. A.* doi:10.1073/pnas.0611547104.

Inoué, S., and Salmon, E. D. (1995). Force generation by microtubule assembly/disassembly in mitosis and related movements. *Mol. Biol. Cell* 6, 1619–1640.

Janke, C., and Kneussel, M. (2010). Tubulin post-translational modifications: Encoding functions on the neuronal microtubule cytoskeleton. *Trends Neurosci.* doi:10.1016/j.tins.2010.05.001.

Janson, M. E., De Dood, M. E., and Dogterom, M. (2003). Dynamic instability of microtubules is regulated by force. *J. Cell Biol.* doi:10.1083/jcb.200301147.

Jozsef, L., Tashiro, K., Kuo, A., Park, E., Skoura, A., Albinsson, S., et al. (2014). Reticulon 4 is necessary for endoplasmic reticulum tubulation, STIM1-Orai1 coupling, and store-operated calcium entry. *J. Biol. Chem.* doi:10.1074/jbc.M114.548602.

Kapitein, L. C., and Hoogenraad, C. C. (2015). Building the Neuronal Microtubule Cytoskeleton. *Neuron* 87, 492–506. doi:10.1016/j.neuron.2015.05.046.

Kiseleva, E., Morozova, K. N., Voeltz, G. K., Allen, T. D., and Goldberg, M. W. (2007). Reticulon 4a/NogoA locates to regions of high membrane curvature and may have a role in nuclear envelope growth. *J. Struct. Biol.* doi:10.1016/j.jsb.2007.08.005.

Kitada, T., Asakawa, S., Hattori, N., Matsumine, H., Yamamura, Y., Minoshima, S., et al. (1998). Mutations in the parkin gene cause autosomal recessive juvenile parkinsonism. *Nature*. doi:10.1038/33416.

Klueg, K. M., Alvarado, D., Muskavitch, M. A. T., and Duffy, J. B. (2002). Creation of a GAL4/UAS-coupled inducible gene expression system for use in Drosophila cultured cell lines. *Genesis*. doi:10.1002/gene.10148.

Koster, G., Van Duijn, M., Hofs, B., and Dogterom, M. (2003). Membrane tube formation from giant vesicles by dynamic association of motor proteins. *Proc. Natl. Acad. Sci. U. S. A.* doi:10.1073/pnas.2531786100.

Kozak, M. (2002). Pushing the limits of the scanning mechanism for initiation of translation. *Gene*. doi:10.1016/S0378-1119(02)01056-9.

Krijnse-Locker, J., Parton, R. G., Fuller, S. D., Griffiths, G., and Dotti, C. G. (1995). The organization of the endoplasmic reticulum and the intermediate compartment in cultured rat hippocampal neurons. *Mol. Biol. Cell*. doi:10.1091/mbc.6.10.1315.

Lacroix, B., Van Dijk, J., Gold, N. D., Guizetti, J., Aldrian-Herrada, G., Rogowski, K., et al. (2010). Tubulin polyglutamylation stimulates spastin-mediated microtubule severing. *J. Cell Biol.* doi:10.1083/jcb.201001024.

Leduc, C., Campàs, O., Zeldovich, K. B., Roux, A., Jolimaitre, P., Bourel-Bonnet, L., et al. (2004). Cooperative extraction of membrane nanotubes by molecular motors. *Proc. Natl. Acad. Sci. U. S. A.* doi:10.1073/pnas.0406598101.

Lee, C., and Chen, L. B. (1988). Dynamic behavior of endoplasmic reticulum in living cells. *Cell*. doi:10.1016/0092-8674(88)90177-8.

Lee, C., Ferguson, M., and Chen, L. B. (1989). Construction of the endoplasmic reticulum. *J. Cell Biol.* doi:10.1083/jcb.109.5.2045.

Li, J., Yan, B., Si, H., Peng, X., Zhang, S. L., and Hu, J. (2017). Atlastin regulates store-operated calcium entry for nerve growth factor-induced neurite outgrowth. *Sci. Rep.* doi:10.1038/srep43490.

Li, M., Zhang, W., Wang, W., He, Q., Yin, M., Qin, X., et al. (2018). Imidazole improves cognition and balances Alzheimer's-like intracellular calcium homeostasis in transgenic Drosophila model. *Neurourol. Urodyn.* doi:10.1002/nau.23448.

Liou, J., Fivaz, M., Inoue, T., and Meyer, T. (2007). Live-cell imaging reveals sequential oligomerization and local plasma membrane targeting of stromal interaction molecule 1 after Ca2+ store depletion. *Proc. Natl. Acad. Sci. U. S. A.* doi:10.1073/pnas.0702866104.

Liou, J., Kim, M. L., Won, D. H., Jones, J. T., Myers, J. W., Ferrell, J. E., et al. (2005). STIM is a Ca2+ sensor essential for Ca2+-store- depletion-triggered Ca2+ influx. *Curr. Biol.* doi:10.1016/j.cub.2005.05.055.

Lo Giudice, T., Lombardi, F., Santorelli, F. M., Kawarai, T., and Orlacchio, A. (2014). Hereditary spastic paraplegia: Clinical-genetic characteristics and evolving molecular mechanisms. *Exp. Neurol.* doi:10.1016/j.expneurol.2014.06.011.

Lu, L., Ladinsky, M. S., and Kirchhausen, T. (2009). Cisternal Organization of the Endoplasmic Reticulum during Mitosis. *Mol. Biol. Cell*. doi:10.1091/mbc.e09-04-0327.

Luik, R. M., Wang, B., Prakriya, M., Wu, M. M., and Lewis, R. S. (2008). Oligomerization of STIM1 couples ER calcium depletion to CRAC channel activation. *Nature*. doi:10.1038/nature07065.

Lumb, J. H., Connell, J. W., Allison, R., and Reid, E. (2012). The AAA ATPase spastin links microtubule severing to membrane modelling. *Biochim. Biophys. Acta - Mol. Cell Res.* doi:10.1016/j.bbamcr.2011.08.010.

Magyar, A., and Váradi, A. (1990). Molecular cloning and chromosomal localization of a sarco/endoplasmic reticulum-type Ca2+-ATPase of drosophila melanogaster. *Biochem. Biophys. Res. Commun.* doi:10.1016/S0006-291X(05)80867-8.

Maléth, J., Choi, S., Muallem, S., and Ahuja, M. (2014). Translocation between PI(4,5)P 2 -poor and PI(4,5)P 2 -rich microdomains during store depletion determines STIM1 conformation and Orai1 gating. *Nat. Commun.* doi:10.1038/ncomms6843.

Mandelkow, E. M., Mandelkow, E., and Milligan, R. A. (1991). Microtubule dynamics and microtubule caps: A time-resolved cryo-electron microscopy study. *J. Cell Biol.* doi:10.1083/jcb.114.5.977.

Mannan, A. U., Boehm, J., Sauter, S. M., Rauber, A., Byrne, P. C., Neesen, J., et al. (2006). Spastin, the most commonly mutated protein in hereditary spastic

paraplegia interacts with Reticulon 1 an endoplasmic reticulum protein. *Neurogenetics*. doi:10.1007/s10048-006-0034-4.

Mattson, M. P. (2004). Pathways towards and away from Alzheimer's disease. *Nature*. doi:10.1038/nature02621.

Mattson, M. R. (2007). Calcium and neurodegeneration. *Aging Cell*. doi:10.1111/j.1474-9726.2007.00275.x.

Maurer, S. P., Fourniol, F. J., Bohner, G., Moores, C. A., and Surrey, T. (2012). EBs recognize a nucleotide-dependent structural cap at growing microtubule ends. *Cell*. doi:10.1016/j.cell.2012.02.049.

McDermott, C. J., Burness, C. E., Kirby, J., Cox, L. E., Rao, D. G., Hewamadduma, C., et al. (2006). Clinical features of hereditary spastic paraplegia due to spastin mutation. *Neurology*. doi:10.1212/01.wnl.0000223315.62404.00.

Michno, K., Knight, D., Campussano, J. M., van de Hoef, D., and Boulianne, G. L. (2009). Intracellular calcium deficits in Drosophila cholinergic neurons expressing wild type or FAD-mutant presenilin. *PLoS One*. doi:10.1371/journal.pone.0006904.

Mockett, R. J., Bayne, A. C. V, Kwong, L. K., Orr, W. C., and Sohal, R. S. (2003). Ectopic expression of catalase in Drosophila mitochondria increases stress resistance but not longevity. *Free Radic. Biol. Med.* doi:10.1016/S0891-5849(02)01190-5.

Montenegro, G., Rebelo, A. P., Connell, J., Allison, R., Babalini, C., D'Aloia, M., et al. (2012). Mutations in the ER-shaping protein reticulon 2 cause the axon-degenerative disorder hereditary spastic paraplegia type 12. *J. Clin. Invest.* doi:10.1172/JCI60560.

Muller, H. J. (1928). The Production of Mutations by X-Rays. *Proc. Natl. Acad. Sci.* doi:10.1073/pnas.14.9.714.

Nakai, J., Ohkura, M., and Imoto, K. (2001). A high signal-to-noise ca2+ probe composed of a single green fluorescent protein. *Nat. Biotechnol.* doi:10.1038/84397.

Nixon-Abell, J., Obara, C. J., Weigel, A. V., Li, D., Legant, W. R., Xu, C. S., et al. (2016). Increased spatiotemporal resolution reveals highly dynamic dense tubular matrices in the peripheral ER. *Science (80-.).* doi:10.1126/science.aaf3928.

Novarino, G., Fenstermaker, A. G., Zaki, M. S., Hofree, M., Silhavy, J. L., Heiberg, A. D., et al. (2014). Exome sequencing links corticospinal motor neuron disease to common neurodegenerative disorders. *Science (80-.).* doi:10.1126/science.1247363.

O'Sullivan, N. C., Jahn, T. R., Reid, E., and O'Kane, C. J. (2012). Reticulon-like-1, the drosophila orthologue of the hereditary spastic paraplegia gene reticulon 2, is required for organization of endoplasmic reticulum and of distal motor axons. *Hum. Mol. Genet.* doi:10.1093/hmg/dds167.

Odde, D. J., Cassimeris, L., and Buettner, H. M. (1995). Kinetics of microtubule catastrophe assessed by probabilistic analysis. *Biophys. J.* doi:10.1016/S0006-3495(95)79953-2.

Oka, T., Hori, M., and Ozaki, H. (2005). Microtubule Disruption Suppresses Allergic Response through the Inhibition of Calcium Influx in the Mast Cell Degranulation Pathway. *J. Immunol.* doi:10.4049/jimmunol.174.8.4584.

Orlacchio, A., Kawarai, T., Rogaeva, E., Song, Y. Q., Paterson, A. D., Bernardi, G., et al. (2002). Clinical and genetic study of a large Italian family linked to SPG12 locus. *Neurology*. doi:10.1212/01.WNL.0000031423.43482.19.

Orlacchio, A., Patrono, C., Gaudiello, F., Rocchi, C., Moschella, V., Floris, R., et al. (2008). Silver syndrome variant of hereditary spastic paraplegia: A locus to 4p and allelism with SPG4. *Neurology*. doi:10.1212/01.wnl.0000294330.27058.61.

Orso, G., Martinuzzi, A., Rossetto, M. G., Sartori, E., Feany, M., and Daga, A. (2005). Disease-related phenotypes in a Drosophila model of hereditary spastic paraplegia are ameliorated by treatment with vinblastine. *J. Clin. Invest.* doi:10.1172/JCI24694.

Orso, G., Pendin, D., Liu, S., Tosetto, J., Moss, T. J., Faust, J. E., et al. (2009). Homotypic fusion of ER membranes requires the dynamin-like GTPase atlastin. *Nature* 460, 978–983. doi:10.1038/nature08886.

Pantakani, D. V. K., Swapna, L. S., Srinivasan, N., and Mannan, A. U. (2008). Spastin oligomerizes into a hexamer and the mutant spastin (E442Q) redistribute the wild-type spastin into filamentous microtubule. *J. Neurochem.* doi:10.1111/j.1471-4159.2008.05414.x.

Park, J., Lee, S. B., Lee, S., Kim, Y., Song, S., Kim, S., et al. (2006). Mitochondrial dysfunction in Drosophila PINK1 mutants is complemented by parkin. *Nature*. doi:10.1038/nature04788.

Park, S. H., Zhu, P. P., Parker, R. L., and Blackstone, C. (2010). Hereditary spastic paraplegia proteins REEP1, spastin, and atlastin-1 coordinate microtubule interactions with the tubular ER network. *J. Clin. Invest.* 120, 1097–1110. doi:10.1172/JCI40979.

Pathak, T., Agrawal, T., Richhariya, S., Sadaf, S., and Hasan, G. (2015). Store-operated calcium entry through Orai is required for transcriptional maturation of the flight circuit in Drosophila. *J. Neurosci.* doi:10.1523/JNEUROSCI.1680-15.2015.

Pendin, D., Greotti, E., Lefkimmiatis, K., and Pozzan, T. (2017). Exploring cells with targeted biosensors. *J. Gen. Physiol.* doi:10.1085/jgp.201611654.

Pendin, D., Greotti, E., and Pozzan, T. (2014). The elusive importance of being a mitochondrial Ca2+ uniporter. *Cell Calcium*. doi:10.1016/j.ceca.2014.02.008.

Penner, R., Fasolato, C., and Hoth, M. (1993). Calcium influx and its control by calcium release. *Curr. Opin. Neurobiol.* doi:10.1016/0959-4388(93)90130-Q.

Perdiz, D., Mackeh, R., Poüs, C., and Baillet, A. (2011). The ins and outs of tubulin acetylation: More than just a post-translational modification? *Cell. Signal.* doi:10.1016/j.cellsig.2010.10.014.

Pizzo, P., Lissandron, V., and Pozzan, T. (2010). The trans-golgi compartment: A new distinct intracellular Ca store. *Commun. Integr. Biol.* doi:10.4161/cib.3.5.12473.

Polymeropoulos, M. H., Lavedan, C., Leroy, E., Ide, S. E., Dehejia, A., Dutra, A., et al. (1997). Mutation in the α-synuclein gene identified in families with Parkinson's disease. *Science (80-.).* doi:10.1126/science.276.5321.2045.

Powers, R. E., Wang, S., Liu, T. Y., and Rapoport, T. A. (2017). Reconstitution of the tubular endoplasmic reticulum network with purified components. *Nature*. doi:10.1038/nature21387.

Prakriya, M., Feske, S., Gwack, Y., Srikanth, S., Rao, A., and Hogan, P. G. (2006). Orai1 is an essential pore subunit of the CRAC channel. *Nature*. doi:10.1038/nature05122.

Puhka, M., Joensuu, M., Vihinen, H., Belevich, I., and Jokitalo, E. (2012). Progressive sheet-to-tubule transformation is a general mechanism for endoplasmic reticulum partitioning in dividing mammalian cells. *Mol. Biol. Cell*. doi:10.1091/mbc.E10-12-0950.

Puhka, M., Vihinen, H., Joensuu, M., and Jokitalo, E. (2007). Endoplasmic reticulum remains continuous and undergoes sheet-to-tubule transformation during cell division in mammalian cells. *J. Cell Biol.* doi:10.1083/jcb.200705112.

Redondo, P. C., Harper, M. T., Rosado, J. A., and Sage, S. O. (2006). A role for cofilin in the activation of store-operated calcium entry by de novo conformational coupling in human platelets. *Blood*. doi:10.1182/blood-2005-05-2015.

Riano, E., Martignoni, M., Mancuso, G., Cartelli, D., Crippa, F., Toldo, I., et al. (2009). Pleiotropic effects of spastin on neurite growth depending on expression levels. *J. Neurochem.* doi:10.1111/j.1471-4159.2009.05875.x.

Rismanchi, N., Soderblom, C., Stadler, J., Zhu, P. P., and Blackstone, C. (2008). Atlastin GTPases are required for Golgi apparatus and ER morphogenesis. *Hum. Mol. Genet.* doi:10.1093/hmg/ddn046.

Rogaev, E. I., Sherrington, R., Rogaeva, E. A., Levesque, G., Ikeda, M., Liang, Y., et al. (1995). Familial Alzheimer's disease in kindreds with missense mutations in a gene on chromosome 1 related to the Alzheimer's disease type 3 gene. *Nature*. doi:10.1038/376775a0.

Roll-Mecak, A., and Vale, R. D. (2005). The Drosophila homologue of the hereditary spastic paraplegia protein, spastin, severs and disassembles microtubules. *Curr. Biol.* doi:10.1016/j.cub.2005.02.029.

Roll-Mecak, A., and Vale, R. D. (2008). Structural basis of microtubule severing by the hereditary spastic paraplegia protein spastin. *Nature*. doi:10.1038/nature06482.

Romero, E., Cha, G. H., Verstreken, P., Ly, C. V., Hughes, R. E., Bellen, H. J., et al. (2008). Suppression of Neurodegeneration and Increased Neurotransmission Caused by Expanded Full-Length Huntingtin Accumulating in the Cytoplasm. *Neuron*. doi:10.1016/j.neuron.2007.11.025.

Roos, J., DiGregorio, P. J., Yeromin, A. V., Ohlsen, K., Lioudyno, M., Zhang, S., et al.

(2005). STIM1, an essential and conserved component of store-operated Ca 2+ channel function. *J. Cell Biol.* doi:10.1083/jcb.200502019.

Roux, A., Cappello, G., Cartaud, J., Prost, J., Goud, B., and Bassereau, P. (2002). A minimal system allowing tubulation with molecular motors pulling on giant liposomes. *Proc. Natl. Acad. Sci. U. S. A.* doi:10.1073/pnas.082107299.

Ruano, L., Melo, C., Silva, M. C., and Coutinho, P. (2014). The global epidemiology of hereditary ataxia and spastic paraplegia: A systematic review of prevalence studies. *Neuroepidemiology*. doi:10.1159/000358801.

Rudolf, R., Mongillo, M., Rizzuto, R., and Pozzan, T. (2003). Looking forward to seeing calcium. *Nat. Rev. Mol. Cell Biol.* doi:10.1038/nrm1153.

S. Tsukita, H. I. (1976). Three-Dimensional Distributionof Smooth Endoplasmic Reticulum in Myelinated Axons. *J. Electron Microsc. (Tokyo).* doi:10.1093/oxfordjournals.jmicro.a050013.

Sanderson, C. M., Connel, J. W., Edwards, T. L., Bright, N. A., Duley, S., Thompson, A., et al. (2006). Spastin and atlastin, two proteins mutated in autosomal-dominant hereditary spastic paraplegia, are binding partners. *Hum. Mol. Genet.* doi:10.1093/hmg/ddi447.

Schaefer, A., Nethe, M., and Hordijk, P. L. (2012). Ubiquitin links to cytoskeletal dynamics, cell adhesion and migration. *Biochem. J.* doi:10.1042/BJ20111815.

Schroeder, L. K., Barentine, A. E. S., Merta, H., Schweighofer, S., Zhang, Y., Baddeley, D., et al. (2019). Dynamic nanoscale morphology of the ER surveyed by STED microscopy. *J. Cell Biol.* doi:10.1083/jcb.201809107.

Schuck, S., Prinz, W. A., Thorn, K. S., Voss, C., and Walter, P. (2009). Membrane expansion alleviates endoplasmic reticulum stress independently of the unfolded protein response. *J. Cell Biol.* doi:10.1083/jcb.200907074.

Schulte, T., Miterski, B., Börnke, C., Przuntek, H., Epplen, J. T., and Schöls, L. (2003). Neurophysiological findings in SPG4 patients differ from other types of spastic paraplegia. *Neurology*. doi:10.1212/01.WNL.0000058769.75218.69.

Schwarz, E. M., and Benzer, S. (1997). Calx, a Na-Ca exchanger gene of Drosophila melanogaster. *Proc. Natl. Acad. Sci. U. S. A.* doi:10.1073/pnas.94.19.10249.

Secondo, A., Bagetta, G., and Amantea, D. (2018). On the Role of Store-Operated Calcium Entry in Acute and Chronic Neurodegenerative Diseases. *Front. Mol. Neurosci.* doi:10.3389/fnmol.2018.00087.

Shaklee, P. M., Idema, T., Koster, G., Storm, C., Schmidt, T., and Dogterom, M. (2008). Bidirectional membrane tube dynamics driven by nonprocessive motors. *Proc. Natl. Acad. Sci. U. S. A.* doi:10.1073/pnas.0709677105.

Sharma, S., Quintana, A., Findlay, G. M., Mettlen, M., Baust, B., Jain, M., et al. (2013). An siRNA screen for NFAT activation identifies septins as coordinators of store-operated Ca2+ entry. *Nature*. doi:10.1038/nature12229.

Shemesh, T., Klemm, R. W., Romano, F. B., Wang, S., Vaughan, J., Zhuang, X., et al. (2014). A model for the generation and interconversion of ER morphologies. *Proc. Natl. Acad. Sci. U. S. A.* doi:10.1073/pnas.1419997111.

Sherrington, R., Rogaev, E. I., Liang, Y., Rogaeva, E. A., Levesque, G., Ikeda, M., et al. (1995). Cloning of a gene bearing missense mutations in early-onset familial Alzheimer's disease. *Nature*. doi:10.1038/375754a0.

Shibata, Y., Shemesh, T., Prinz, W. A., Palazzo, A. F., Kozlov, M. M., and Rapoport, T. A. (2010). Mechanisms determining the morphology of the peripheral ER. *Cell*. doi:10.1016/j.cell.2010.11.007.

Shibata, Y., Voeltz, G. K., and Rapoport, T. A. (2006). Rough Sheets and Smooth Tubules. *Cell*. doi:10.1016/j.cell.2006.07.019.

Shibata, Y., Voss, C., Rist, J. M., Hu, J., Rapoport, T. A., Prinz, W. A., et al. (2008). The reticulon and Dp1/Yop1p proteins form immobile oligomers in the tubular endoplasmic reticulum. *J. Biol. Chem.* doi:10.1074/jbc.M800986200.

Simon, A. F., Liang, D. T., and Krantz, D. E. (2006). Differential decline in behavioral performance of Drosophila melanogaster with age. *Mech. Ageing Dev.* doi:10.1016/j.mad.2006.02.006.

Smyth, J. T., DeHaven, W. I., Bird, G. S., and Putney, J. W. (2007). Role of the microtubule cytoskeleton in the function of the store-operated Ca2+ channel activator STIM1. *J. Cell Sci.* doi:10.1242/jcs.015735.

Soboloff, J., Rothberg, B. S., Madesh, M., and Gill, D. L. (2012). STIM proteins: Dynamic

calcium signal transducers. *Nat. Rev. Mol. Cell Biol.* doi:10.1038/nrm3414.

Solowska, J. M., Garbern, J. Y., and Baas, P. W. (2010). Evaluation of loss of function as an explanation for SPG4-based hereditary spastic paraplegia. *Hum. Mol. Genet.* doi:10.1093/hmg/ddq177.

Southall, T. D., Terhzaz, S., Cabrero, P., Chintapalli, V. R., Evans, J. M., Dow, J. A. T., et al. (2006). Novel subcellular locations and functions for secretory pathway Ca 2+/Mn2+-ATPases. *Physiol. Genomics*. doi:10.1152/physiolgenomics.00038.2006.

Sparkes, I., Tolley, N., Aller, I., Svozil, J., Osterrieder, A., Botchway, S., et al. (2010). Five Arabidopsis reticulon isoforms share endoplasmic reticulum location, topology, and membrane-shaping properties. *Plant Cell*. doi:10.1105/tpc.110.074385.

Spillantini, M. G., Schmidt, M. L., Lee, V. M. Y., Trojanowski, J. Q., Jakes, R., and Goedert, M. (1997). α-synuclein in Lewy bodies [8]. *Nature*. doi:10.1038/42166.

Stocker, H., and Gallant, P. (2008). Getting started : an overview on raising and handling Drosophila. *Methods Mol. Biol.*

Summerville, J. B., Faust, J. F., Fan, E., Pendin, D., Daga, A., Formella, J., et al. (2016). The effects of ER morphology on synaptic structure and function in Drosophila melanogaster . *J. Cell Sci.* doi:10.1242/jcs.184929.

Takeshima, H., Nishi, M., Iwabe, N., Miyata, T., Hosoya, T., Masai, I., et al. (1994). Isolation and characterization of a gene for a ryanodine receptor/calcium release channel in Drosophila melanogaster. *FEBS Lett.* doi:10.1016/0014-5793(94)80634-9.

Tang, T. S., Slow, E., Lupu, V., Stavrovskaya, I. G., Sugimori, M., Llinás, R., et al. (2005). Disturbed Ca2+ signalling and apoptosis of medium spiny neurons in Huntington's disease. *Proc. Natl. Acad. Sci. U. S. A.* doi:10.1073/pnas.0409402102.

Terasaki, M. (2018). Axonal endoplasmic reticulum is very narrow. *J. Cell Sci.* doi:10.1242/jcs.210450.

Terasaki, M., Chen, L. B., and Fujiwara, K. (1986). Microtubules and the endoplasmic reticulum are highly interdependent structures. *J. Cell Biol.* doi:10.1083/jcb.103.4.1557.

Terasaki, M., and Jaffe, L. A. (1991). Organization of the sea urchin egg endoplasmic reticulum and its reorganization at fertilization. *J. Cell Biol.* doi:10.1083/jcb.114.5.929.

Terasaki, M., and Reese, T. S. (1994). Interactions among endoplasmic reticulum, microtubules, and retrograde movements of the cell surface. *Cell Motil. Cytoskeleton*. doi:10.1002/cm.970290402.

Terasaki, M., Runft, L. L., and Hand, A. R. (2001). Changes in Organization of the Endoplasmic Reticulum during Xenopus Oocyte Maturation and Activation. *Mol. Biol. Cell*. doi:10.1091/mbc.12.4.1103.

Terasaki, M., Shemesh, T., Kasthuri, N., Klemm, R. W., Schalek, R., Hayworth, K. J., et al. (2013). XStacked endoplasmic reticulum sheets are connected by helicoidal membrane motifs. *Cell*. doi:10.1016/j.cell.2013.06.031.

Tolley, N., Sparkes, I. A., Hunter, P. R., Craddock, C. P., Nuttall, J., Roberts, L. M., et al. (2008). Overexpression of a plant reticulon remodels the lumen of the cortical endoplasmic reticulum but does not perturb protein transport. *Traffic*. doi:10.1111/j.1600-0854.2007.00670.x.

Tran, P. T., Walker, R. A., and Salmon, E. D. (1997). A metastable intermediate state of microtubule dynamic instability that differs significantly between plus and minus ends. *J. Cell Biol.* doi:10.1083/jcb.138.1.105.

Tsai, F. C., Seki, A., Yang, H. W., Hayer, A., Carrasco, S., Malmersjö, S., et al. (2014). A polarized Ca2+, diacylglycerol and STIM1 signalling system regulates directed cell migration. *Nat. Cell Biol.* doi:10.1038/ncb2906.

Tsien, R. Y. (1980). New Calcium Indicators and Buffers with High Selectivity Against Magnesium and Protons: Design, Synthesis, and Properties of Prototype Structures. *Biochemistry*. doi:10.1021/bi00552a018.

Tsien, R. Y., Pozzan, T., and Rink, T. J. (1982). Calcium homeostasis in intact lymphocytes: Cytoplasmic free calcium monitored with a intracellularly trapped fluorescent indicator. *J. Cell Biol.* doi:10.1083/jcb.94.2.325.

Valenstein, M. L., and Roll-Mecak, A. (2016). Graded Control of Microtubule Severing by Tubulin Glutamylation. *Cell*. doi:10.1016/j.cell.2016.01.019.

Valente, E. M., Abou-Sleiman, P. M., Caputo, V., Muqit, M. M. K., Harvey, K., Gispert, S., et al. (2004). Hereditary early-onset Parkinson's disease caused by mutations in PINK1. *Science (80-.).* doi:10.1126/science.1096284.

Vedrenne, C., and Hauri, H. P. (2006). Morphogenesis of the endoplasmic reticulum: Beyond active membrane expansion. *Traffic*. doi:10.1111/j.1600-0854.2006.00419.x.

Venkiteswaran, G., and Hasan, G. (2009). Intracellular Ca2+ signaling and store-operated Ca2+ entry are required in Drosophila neurons for flight. *Proc. Natl. Acad. Sci.* doi:10.1073/pnas.0902982106.

Vig, M., Beck, A., Billingsley, J. M., Lis, A., Parvez, S., Peinelt, C., et al. (2006a). CRACM1 Multimers Form the Ion-Selective Pore of the CRAC Channel. *Curr. Biol.* doi:10.1016/j.cub.2006.08.085.

Vig, M., Peinelt, C., Beck, A., Koomoa, D. L., Rabah, D., Koblan-Huberson, M., et al. (2006b). CRACM1 is a plasma membrane protein essential for store-operated Ca 2+ entry. *Science (80-.).* doi:10.1126/science.1127883.

Voeltz, G. K., Prinz, W. A., Shibata, Y., Rist, J. M., and Rapoport, T. A. (2006). A class of membrane proteins shaping the tubular endoplasmic reticulum. *Cell*. doi:10.1016/j.cell.2005.11.047.

Walker, R. A., O'Brien, E. T., Pryer, N. K., Soboeiro, M. F., Voter, W. A., Erickson, H. P., et al. (1988). Dynamic instability of individual microtubules analyzed by video light microscopy: rate constants and transition frequencies. *J. Cell Biol.* doi:10.1083/jcb.107.4.1437.

Walkinshaw, E., Gai, Y., Farkas, C., Richter, D., Nicholas, E., Keleman, K., et al. (2015). Identification of genes that promote or inhibit olfactory memory formation in Drosophila. *Genetics*. doi:10.1534/genetics.114.173575.

Wandosell, F., Serrano, L., and Avila, J. (1987). Phosphorylation of alpha-tubulin carboxyl-terminal tyrosine prevents its incorporation into microtubules. *J. Biol. Chem.*

Wangler, M. F., Yamamoto, S., and Bellen, H. J. (2015). Fruit flies in biomedical research. *Genetics*. doi:10.1534/genetics.114.171785.

Waterman-Storer, C. M., Gregory, J., Parsons, S. F., and Salmon, E. D. (1995). Membrane/microtubule tip attachment complexes (TACs) allow the assembly dynamics of plus ends to push and pull membranes into tubulovesicular networks in interphase Xenopus egg extracts. *J. Cell Biol.* 130, 1161–1169. doi:10.1083/jcb.130.5.1161.

Waterman-Storer, C. M., and Salmon, E. D. (1998). Endoplasmic reticulum membrane tubules are distributed by microtubules in living cells using three distinct mechanisms. *Curr. Biol.* 8, 798–807. doi:10.1016/s0960-9822(98)70321-5.

West, M., Zurek, N., Hoenger, A., and Voeltz, G. K. (2011). A 3D analysis of yeast ER structure reveals how ER domains are organized by membrane curvature. *J. Cell Biol.* doi:10.1083/jcb.201011039.

White, S. R., Evans, K. J., Lary, J., Cole, J. L., and Lauring, B. (2007). Recognition of C-terminal amino acids in tubulin by pore loops in Spastin is important for microtubule severing. *J. Cell Biol.* doi:10.1083/jcb.200610072.

Witte, H., Neukirchen, D., and Bradke, F. (2008). Microtubule stabilization specifies initial neuronal polarization. *J. Cell Biol.* doi:10.1083/jcb.200707042.

Wloga, D., and Gaertig, J. (2010). Post-translational modifications of microtubules. *J. Cell Sci.* doi:10.1242/jcs.063727.

Woo, J. S., Srikanth, S., Nishi, M., Ping, P., Takeshima, H., and Gwack, Y. (2016). Junctophilin-4, a component of the endoplasmic reticulum–plasma membrane junctions, regulates Ca 2+ dynamics in T cells . *Proc. Natl. Acad. Sci.* doi:10.1073/pnas.1524229113.

Woźniak, M. J., Bola, B., Brownhill, K., Yang, Y. C., Levakova, V., and Allan, V. J. (2009). Role of kinesin-1 and cytoplasmic dynein in endoplasmic reticulum movement in VERO cells. *J. Cell Sci.* doi:10.1242/jcs.041962.

Wu, M. M., Buchanan, J., Luik, R. M., and Lewis, R. S. (2006). Ca 2+ store depletion causes STIM1 to accumulate in ER regions closely associated with the plasma membrane. *J. Cell Biol.* doi:10.1083/jcb.200604014.

Yajima, H., Ogura, T., Nitta, R., Okada, Y., Sato, C., and Hirokawa, N. (2012). Conformational changes in tubulin in GMPCPP and GDP-taxol microtubules

observed by cryoelectron microscopy. *J. Cell Biol.* doi:10.1083/jcb.201201161.

Yalçın, B., Zhao, L., Stofanko, M., O'Sullivan, N. C., Kang, Z. H., Roost, A., et al. (2017). Modeling of axonal endoplasmic reticulum network by spastic paraplegia proteins. *Elife*. doi:10.7554/eLife.23882.

Yeromin, A. V., Zhang, S. L., Jiang, W., Yu, Y., Safrina, O., and Cahalan, M. D. (2006). Molecular identification of the CRAC channel by altered ion selectivity in a mutant of Orai. *Nature*. doi:10.1038/nature05108.

Yoshihara, M., Ensminger, A. W., and Littleton, J. T. (2001). Neurobiology and the Drosophila genome. *Funct. Integr. Genomics*. doi:10.1007/s101420000029.

Yoshikawa, S., Tanimura, T., Miyawaki, A., Nakamura, M., Yuzaki, M., Furuichi, T., et al. (1992). Molecular cloning and characterization of the inositol 1,4,5-trisphosphate receptor in Drosophila melanogaster. *J. Biol. Chem.*

Zhang, R., Alushin, G. M., Brown, A., and Nogales, E. (2015). Mechanistic origin of microtubule dynamic instability and its modulation by EB proteins. *Cell*. doi:10.1016/j.cell.2015.07.012.

Zhang, S. L., Yeromin, A. V., Zhang, X. H.-F., Yu, Y., Safrina, O., Penna, A., et al. (2006a). Genome-wide RNAi screen of Ca2+ influx identifies genes that regulate Ca2+ release-activated Ca2+ channel activity. *Proc. Natl. Acad. Sci.* doi:10.1073/pnas.0603161103.

Zhang, S. L., Yeromin, A. V., Zhang, X. H. F., Yu, Y., Safrina, O., Penna, A., et al. (2006b). Genome-wide RNAi screen of Ca2+ influx identifies genes that regulate Ca2+ release-activated Ca2+ channel activity. *Proc. Natl. Acad. Sci. U. S. A.* doi:10.1073/pnas.0603161103.

Zhang, S. L., Yu, Y., Roos, J., Kozak, J. A., Deerinck, T. J., Ellisman, M. H., et al. (2005). STIM1 is a Ca2+ sensor that activates CRAC channels and migrates from the Ca2+ store to the plasma membrane. *Nature*. doi:10.1038/nature04147.

Zimm, D. L. G. (1992). *The Genome of Drosophila Melanogaster 1st Edition*.

Zurek, N., Sparks, L., and Voeltz, G. (2011). Reticulon short hairpin transmembrane domains are used to shape ER tubules. *Traffic*. doi:10.1111/j.1600-0854.2010.01134.x.